Energy Economics 160 (2026) 109478

Contents lists available at ScienceDirect

Energy Economics

journal homepage: www.elsevier.com/locate/eneco

Speculative price dynamics in a cobweb-type oil market model[☆,☆☆]

Laura Gardini [a,b], Davide Radi [b,c], Iryna Sushko [c,d], Frank Westerhoff [e,*]

[a] Dept. of Economics, Society and Politics, University of Urbino Carlo Bo, Italy
[b] Dept. of Finance, VŠB - Technical University of Ostrava, Ostrava, Czech Republic
[c] Dept. of Mathematics for Economic, Financial and Actuarial Sciences, Catholic University of the Sacred Heart, Milan, Italy
[d] Inst. of Mathematics, NAS of Ukraine, Kyiv, Ukraine
[e] Dept. of Economics, University of Bamberg, Germany

ARTICLE INFO

JEL classification:
C63
D84
Q41

Keywords:
Complex oil price dynamics
Speculative behavior
Basis-trade arbitrage
Regulatory policies
Cobweb-type model
Discontinuous piecewise linear maps
Stability and bifurcation analysis

ABSTRACT

We develop a cobweb-type oil market model in which producers' supply responds positively to the lagged oil price, while consumers' demand responds negatively to the current oil price. In addition, speculators buy or sell oil to maintain a desired market position and to exploit basis-trade arbitrage opportunities. In the absence of speculators, the oil price, governed by a one-dimensional linear map, converges to its fundamental value when the slope of the consumers' demand schedule exceeds that of the producers' supply schedule. When speculators are present, the oil price is determined by a two-dimensional discontinuous piecewise linear map, and both regular and irregular price movements may occur regardless of the relationship between the slopes of the consumers' demand and producers' supply schedules. The model reproduces key stylized facts of oil markets, including their excessive volatility and pronounced boom–bust cycles. We also address questions related to regulatory policy.

1. Introduction

Numerous models with heterogeneous interacting agents have been developed in recent years to study the speculative dynamics of stock and foreign exchange markets. Seminal contributions include (Day and Huang, 1990; Chiarella, 1992; De Grauwe et al., 1993; Brock and Hommes, 1998), while comprehensive reviews are provided by Hommes (2013), Dieci and He (2018), and Axtell and Farmer (2025). These models demonstrate that nonlinear interactions between heterogeneous agents following simple trading rules may generate complex price dynamics. Due to their explanatory power, such models are also applied in policy analysis; see He and Westerhoff (2005), Anufriev and Tuinstra (2013), and Dieci et al. (2022) for examples, as well as Westerhoff (2008) and Westerhoff and Franke (2018) for reviews. It is noteworthy that the supply of the underlying assets in these models is typically assumed to be constant. While this simplifying assumption appears reasonable for stock and foreign exchange markets, it is less appropriate for commodity markets.

Building on this strand of literature, this paper proposes a stock-flow consistent model with heterogeneous interacting agents that sheds light on the speculative dynamics of the oil market. Unlike related models of equity and foreign exchange markets, the underlying asset in our model — oil — is produced and consumed in every period. To capture this characteristic, we construct a cobweb-type model of the oil market. As is common in this line of research, we assume that producers' supply of oil increases with past oil prices, whereas consumers' demand for oil decreases with the current oil price. Assuming market clearing and linear demand and supply schedules, the oil price, governed by a one-dimensional linear map, converges to its fundamental value when the slope of the consumers' demand schedule exceeds that of the producers' supply schedule; otherwise, the price diverges in a zigzag manner. This well-known property of cobweb models was already noted by Ricci (1930), Schultz (1930), Tinbergen (1930), and

☆ This article is part of a Special issue entitled: 'Climate Change and Green Transition' published in Energy Economics.
☆☆ This paper was presented at the 28th Annual Workshop on Economics with Heterogeneous Interacting Agents (WEHIA 2025), held at Queen Mary University of London. We thank the participants for their helpful comments, in particular Paolo Zeppini, as well as the anonymous referees and the handling editor, Boqiang Lin, for their constructive suggestions.
* Correspondence to: Feldkirchenstrasse 21, 96052 Bamberg, Germany.
E-mail address: frank.westerhoff@uni-bamberg.de (F. Westerhoff).

https://doi.org/10.1016/j.eneco.2026.109478
Received 29 September 2025; Received in revised form 4 June 2026; Accepted 23 June 2026
Available online 27 June 2026

Leontief (1934), and was termed the "Cobweb Theorem" in Ezekiel's (1938) survey on the origins of commodity price fluctuations.[1] Moreover, we show that policymakers can increase the steady-state oil price, reduce steady-state oil consumption, and enhance market stability by imposing higher tax rates on producers' oil revenues. Given the growing urgency of climate change, such policy implications would appear highly valuable. However, speculators also influence the oil market.

To capture their impact on the oil market in a stylized manner, we assume that speculators buy or sell oil in order to maintain a desired market position and to conduct arbitrage through optimal basis trades. This assumption further implies that speculators are able to store oil, albeit only to a limited extent. Stock-flow consistency requires that speculators' positions in the oil market cannot be negative. Consequently, the oil price is driven by a two-dimensional discontinuous piecewise linear map. Amongst others, we show that Ezekiel's (1938) "Cobweb Theorem" no longer holds in the presence of speculators. Regardless of the relationship between the slopes of the consumers' demand and producers' supply schedules, both regular and irregular oil price dynamics may arise. Moreover, our analysis reveals that imposing a tax on producers' oil revenues provides policymakers with only limited control over oil market dynamics.[2] The robustness of our main findings is assessed through a number of model extensions, including an upper bound on speculators' oil storage capacity, heterogeneous forecasting rules, adaptive learning mechanisms, and a population of heterogeneous speculators governed by the large-type-limit framework proposed in Brock et al. (2005). Furthermore, by introducing demand and supply shocks, we also identify mechanisms that can generate bubbles, crashes, excess volatility, and volatility bursts, as observed in the real oil markets. Finally, a calibration exercise based on WTI crude oil price data shows that the model replicates the main statistical properties of oil price fluctuations for parameter configurations under which the deterministic skeleton of the model exhibits either cyclical or chaotic dynamics.

Two further remarks are in order. First, a number of piecewise linear models — whether continuous or discontinuous — have recently been proposed that, owing to their analytical tractability, offer clear-cut insights into the functioning of economic systems that would otherwise be difficult to obtain. For financial market applications, we refer the reader to Tramontana et al. (2013), Panchuk et al. (2018), Jungeilges et al. (2021, 2022), Gardini et al. (2022, 2025), and Sushko and Tramontana (2025). Mathematical tools for analyzing such systems are discussed in Zhusubaliyev and Mosekilde (2003), di Bernardo et al. (2008), and Avrutin et al. (2019). Second, there are a few related papers that study the speculative dynamics of commodity markets. Cutler et al. (1990, 1991) develop a model of asset market equilibrium in which interactions between rational investors and feedback traders mimic certain stylized facts of commodity markets. In contrast, the commodity market model by Reitz and Westerhoff (2007) emphasizes interactions between chartists and fundamentalists. Sornette et al. (2009) employ such models to predict major turning points in the price dynamics of oil markets. ter Ellen and Zwinkels (2010) propose a chartist–fundamentalist model in which the oil price adjusts in response to excess demand-driven by the speculative orders of chartists and fundamentalists, as well as the net real demand of consumers and producers.[3] This model most closely resembles ours, although we assume a stock–flow consistent setup instead of a disequilibrium approach. Our paper aims to contribute to these strands of research as well.

We proceed as follows. In Section 2, we develop a simple cobweb-type model of the oil market in which speculators' oil positions are constrained to be nonnegative. In Section 3, we present several model extensions, including the introduction of an upper bound on speculators' oil holdings. In Section 4, we examine effects of demand and supply shocks. Section 5 concludes. Detailed derivations and proofs of the main results are provided in Appendices A and B. Appendix C provides an alternative foundation for speculators' optimal short-run position in the oil market, while Appendix D develops a learning-based microfoundation for the extrapolative expectations rule.

2. A simple cobweb-type oil market model

The oil price in period $t+1$, denoted by P_{t+1}, is determined by the behavior of four types of agents: producers, speculators, consumers, and policymakers. We briefly outline their key activities and clarify the time structure of our model. Due to a one-period production lag, producers' oil supply in period $t+1$, denoted by S_{t+1}, depends on their oil price expectations. Assuming naïve expectations and profit maximization subject to a quadratic cost function, producers' oil supply in period $t+1$ increases linearly with the oil price in period t. Owing to long-run portfolio considerations, speculators hold a positive position in the oil market when the oil price equals its fundamental value.[4] In the short run, however, their desired position for period $t+1$ also depends on arbitrage opportunities in the spot–futures basis. To enhance this arbitrage, speculators buy or sell oil from storage, thereby affecting aggregate oil demand and supply. The speculators' oil demand or supply is denoted by Δ_{t+1}. Consumer demand in period $t+1$, denoted by D_{t+1}, depends linearly on the oil price in that same period. In each period, the oil price adjusts to ensure market clearing. Policymakers may impose a tax on producers' oil revenues with the aim of reducing oil consumption by increasing the oil price, though the impact of such a tax on oil price dynamics is non-trivial.

2.1. Setup

Let us turn to the details of our oil market model. Market clearing in the oil market requires that

$$D_{t+1} + \Delta_{t+1} = S_{t+1}. \tag{1}$$

Consumer demand for oil decreases linearly with the oil price and is specified as

$$D_{t+1} := a - bP_{t+1}, \tag{2}$$

where a and b are positive demand parameters. Producers face a one-period production lag and incur quadratic costs (see Dieci and Westerhoff (2010) for similar assumptions), described by the cost function

$$C_{t+1} := \frac{1}{2c'} S_{t+1}^2. \tag{3}$$

Note that an increase in the inverse cost parameter $c' > 0$ reflects lower marginal production costs. Risk-neutral producers determine their optimal oil supply by maximizing expected profits, defined as

$$E_{o,t}\left[\pi_{t+1}\right] = (1-\tau)\, E_{o,t}\left[P_{t+1}\right] S_{t+1} - \frac{1}{2c'} S_{t+1}^2, \tag{4}$$

[1] A few decades later, it became evident that certain nonlinear variants of the cobweb model can generate chaotic cobweb dynamics. See Artstein (1983), Chiarella (1988), and Hommes (1991) for early examples.

[2] A word of caution is in order. The policy results derived in this paper are model-specific and should not be interpreted as general statements about real-world oil markets. Moreover, policymakers may have additional instruments at their disposal that could stabilize the dynamics within our framework.

[3] ter Ellen et al. (2021) compare the extent of behavioral heterogeneity across different asset classes.

[4] In practice, large commodity trading firms such as Vitol and Glencore may hold non-zero net positions even in the absence of apparent mispricing, reflecting their role as intermediaries in physical oil markets and their engagement in storage and spot–futures arbitrage.

where $0 \le \tau < 1$ represents a revenue tax, imposed by policymakers. Assuming naïve expectations, producers form their oil price forecast as follows:

$$E_{o,t}\left[P_{t+1}\right] = P_t. \tag{5}$$

The resulting optimal oil supply of producers in period $t+1$ is then given by

$$S_{t+1} = cP_t, \tag{6}$$

where $c = (1-\tau)c' > 0$. Accordingly, producers' oil supply in period $t+1$ decreases with the tax rate and increases with the inverse cost parameter and the oil price in period t.

Let us briefly discuss an important benchmark model. In the absence of speculators, that is, when $\Delta_{t+1} = 0$, the oil price follows the one-dimensional linear map

$$P_{t+1} = \frac{a}{b} - \frac{c}{b}P_t. \tag{7}$$

The steady-state oil price, denoted by $\bar{P} = \frac{a}{b+c}$, is globally stable provided that $c < b$. Specifically, if $c < b$, the oil price converges to its steady state in a zigzag manner; if $c > b$, the oil price follows an explosive zigzag path. Only in the limiting case $c = b$ does the oil price exhibit constant zigzag dynamics. These three scenarios correspond to the classical "Cobweb Theorem", originally established by Ricci (1930), Schultz (1930), Tinbergen (1930), and Leontief (1934), and later synthesized by Ezekiel (1938). They serve as useful benchmarks for our further analysis. At the steady state, oil consumption equals $\bar{D} = a - b\bar{P} = \frac{ac}{b+c}$. Hence, the impact of the revenue tax rate is clear in the absence of speculators: higher tax rates raise the steady-state oil price, reduce steady-state oil consumption, and enhance market stability.

In the following, we regard the fundamental value of the oil market as $F = \bar{P}$. Indeed, the steady-state oil price is determined solely by structural demand and supply parameters. Expressed in deviations from this fundamental value, i.e., by defining $x_{t+1} = P_{t+1} - F$, the law of motion becomes

$$x_{t+1} = -\frac{c}{b}x_t, \tag{8}$$

with steady state $\bar{x} = 0$. Needless to say, the condition for global stability of this steady state remains $c < b$.

We capture the market impact of speculators as follows. Let δ_{t+1} and δ_t stand for speculators' desired positions in the oil market in periods $t+1$ and t, respectively. Speculators' demand or supply of oil in period $t+1$ results as

$$\Delta_{t+1} = \delta_{t+1} - \delta_t. \tag{9}$$

If speculators' desired position in period $t+1$ is lower than in period t, they buy oil; if it is higher, they sell oil. Speculators exert no influence on the oil market when their desired position remains constant across two consecutive periods. As we will see, equilibrium and out-of-equilibrium constellations may lead to this outcome.

Speculators' desired position in the oil market comprises a long-term portfolio position and a short-term speculative position. The long-term portfolio position reflects a portfolio diversification decision made at the organizational level, outside the direct control of the speculators themselves. We assume here that the speculators operate within a larger trading house for which it is optimal (for reasons exogenous to the model) to hold a certain amount of oil, denoted by $h > 0$.[5] The short-term speculative position, denoted by $\tilde{\delta}_{t+1}$, reflects the speculators' desire to earn additional profits through short-term trading. In total, the speculator's desired position in the oil market is given by

$$\delta_{t+1} = h + \tilde{\delta}_{t+1}. \tag{10}$$

To ensure stock-flow consistency, we impose the restriction $\delta_{t+1} \ge 0$, which prevents speculators from selling more oil from storage than they currently possess. While the trading house allows that speculators' position in the oil market may deviate from h in the short run, in the long run, when the oil price reflects its fundamental value, $\tilde{\delta}_{t+1}$ must equal zero.

The short-term speculative demand component arises from cash-and-carry and reverse cash-and-carry arbitrage (i.e., basis trading), see, e.g., Ederington et al. (2021). In particular, net of storage and transportation costs, professional traders have an incentive to store oil at time $t+1$ whenever the spot price is lower than the corresponding oil futures price and sell it otherwise. Since we focus on short-term speculators, these operations exploit only the misalignment between the spot price at time $t+1$, denoted by P_{t+1}, and the one-period-ahead futures price, denoted by $P_{f,t+2}$.

Regarding the oil futures market, we assume that future oil price is consistent with speculators' expectations about the oil price at time $t+2$, that is,

$$P_{f,t+2} = E_{s,t}\left[P_{t+2}\right]. \tag{11}$$

Moreover, we assume that storage and transportation generate a quadratic carrying-cost function with respect to the speculative position z_{t+1}:

$$C_s\left(z_{t+1}\right) = \frac{\alpha}{2}\left(z_{t+1}\right)^2 + f, \tag{12}$$

where $\alpha > 0$ measures marginal transportation costs and f denotes storage-infrastructure costs.

Accordingly, speculators' profits from cash-and-carry arbitrage strategy, see, e.g., Ederington et al. (2021), are given by

$$\pi_{t+2} = \left(P_{f,t+2} - P_{t+1}\right)z_{t+1} - C_s\left(z_{t+1}\right). \tag{13}$$

Hence, the optimal basis-trade position is obtained by solving

$$\tilde{\delta}_{t+1} = \arg\max_{z_{t+1}} \pi_{t+2}. \tag{14}$$

and by standard first-order and second-order conditions, we have

$$\tilde{\delta}_{t+1} = \frac{E_{s,t}\left[P_{t+2} - P_{t+1}\right]}{\alpha}. \tag{15}$$

Following Day and Huang (1990) regarding speculators' expectation formation, we assume that expected gains from basis trading are proportional to the deviation of the oil price from its fundamental value F:

$$E_{s,t}\left[P_{t+2} - P_{t+1}\right] = \beta\left(P_t - F\right). \tag{16}$$

where $\beta > 0$.[6] Substituting into (15) yields the speculators' optimal short-term position in the oil market is

$$\tilde{\delta}_{t+1} = d\left(P_t - F\right), \tag{17}$$

where $d = \frac{\beta}{\alpha} > 0$. Hence, speculators increase their oil holdings when the market becomes more bullish, i.e., when the current oil price exceeds its fundamental benchmark.[7]

Since speculators desired (total) position in the oil market cannot become negative, we arrive at

$$\delta_{t+1} = \begin{cases} h + d\left(P_t - F\right) & \text{if} \quad h + d\left(P_t - F\right) > 0 \\ 0 & \text{if} \quad h + d\left(P_t - F\right) \le 0 \end{cases}. \tag{18}$$

[5] In addition to the benefits of portfolio diversification, holding a positive position in the oil market may also serve as an inflation hedge, as discussed in more detail by Markowitz (1952), Froot (1995), Lin et al. (2014), Okorie and Lin (2020) and Neville et al. (2021).

[6] Several alternative forecasting rules are considered in the following.

[7] Appendix C provides an alternative derivation, based on mean–variance portfolio theory, of the same optimal short-term speculative position in the oil market given in (17).

$$A := \begin{cases} P_{t+1} = \begin{cases} -\frac{c}{b}P_t + \frac{a}{b} & \text{if} \quad h + d\left(P_t - F\right) \le 0 \wedge h + d\left(Y_t - F\right) \le 0 \\ -\frac{c}{b}P_t - \frac{d}{b}\left(Y_t - F\right) - \frac{h}{b} + \frac{a}{b} & \text{if} \quad h + d\left(P_t - F\right) \le 0 \wedge h + d\left(Y_t - F\right) > 0 \\ -\frac{c}{b}P_t + \frac{d}{b}\left(P_t - F\right) + \frac{h}{b} + \frac{a}{b} & \text{if} \quad h + d\left(P_t - F\right) > 0 \wedge h + d\left(Y_t - F\right) \le 0 \\ -\frac{c}{b}P_t + \frac{d}{b}\left(P_t - Y_t\right) + \frac{a}{b} & \text{if} \quad h + d\left(P_t - F\right) > 0 \wedge h + d\left(Y_t - F\right) > 0 \end{cases}, \\ Y_{t+1} = P_t \end{cases} \tag{20}$$

Box I.

$$B := \begin{cases} x_{t+1} = \begin{cases} f_1\left(x_t, y_t\right) := -\frac{c}{b}x_t & \text{if} \quad \left(x_t, y_t\right) \in \mathcal{B}_1 := \left\{ \left(x_t, y_t\right) \middle| x_t \le -\frac{h}{d} \wedge y_t \le -\frac{h}{d} \right\} \\ f_2\left(x_t, y_t\right) := -\frac{c}{b}x_t - \frac{d}{b}y_t - \frac{h}{b} & \text{if} \quad \left(x_t, y_t\right) \in \mathcal{B}_2 := \left\{ \left(x_t, y_t\right) \middle| x_t \le -\frac{h}{d} \wedge y_t > -\frac{h}{d} \right\} \\ f_3\left(x_t, y_t\right) := -\frac{c-d}{b}x_t + \frac{h}{b} & \text{if} \quad \left(x_t, y_t\right) \in \mathcal{B}_3 := \left\{ \left(x_t, y_t\right) \middle| x_t > -\frac{h}{d} \wedge y_t \le -\frac{h}{d} \right\} \\ f_4\left(x_t, y_t\right) := -\frac{c-d}{b}x_t - \frac{d}{b}y_t & \text{if} \quad \left(x_t, y_t\right) \in \mathcal{B}_4 := \left\{ \left(x_t, y_t\right) \middle| x_t > -\frac{h}{d} \wedge y_t > -\frac{h}{d} \right\} \end{cases}, \\ y_{t+1} = x_t \end{cases} \tag{21}$$

Box II.

Note that (18) encompasses two generic cases. When speculators are highly pessimistic about the future oil price, i.e., when $P_t - F \le -\frac{h}{d}$, they will refrain from holding any oil. Otherwise, their speculative oil holding is positive, and the desired position in the oil market increases with the oil price, reflecting growing optimism in bullish markets.

The switching boundary in the piecewise linear demand function (18) ensures that speculators cannot sell more oil from their storage than they possess. This is consistent with the physical oil market, where short-selling of the commodity is not feasible, in contrast to futures markets. Since δ_{t+1} is piecewise defined with two branches, the relation $\Delta_{t+1} = \delta_{t+1} - \delta_t$ yields a total of four branches, given by

$$\Delta_{t+1} = \begin{cases} 0 & \text{if} \quad P_t - F \le -\frac{h}{d} \wedge P_{t-1} - F \le -\frac{h}{d} \\ -h - d\left(P_{t-1} - F\right) & \text{if} \quad P_t - F \le -\frac{h}{d} \wedge P_{t-1} - F > -\frac{h}{d} \\ h + d\left(P_t - F\right) & \text{if} \quad P_t - F > -\frac{h}{d} \wedge P_{t-1} - F \le -\frac{h}{d} \\ d\left(P_t - Y_{t-1}\right) & \text{if} \quad P_t - F > -\frac{h}{d} \wedge P_{t-1} - F > -\frac{h}{d} \end{cases}. \tag{19}$$

Although our modeling of the market impact of speculators is simple, it encompasses different trading behaviors. If speculators are pessimistic in both of the last two trading periods, they do not trade. If they are pessimistic in only one of the last two trading periods, they either deplete their oil position or build a new one. If speculators are not too pessimistic in either of the last two trading periods, they operate as trend extrapolators. This structure carries over to the dynamics of our oil market model, which are governed by the following two-dimensional discontinuous piecewise linear map (see Eq. (20) in Box I) where $Y_{t+1} = P_t$ is an auxiliary variable. By defining $x_{t+1} = P_{t+1} - F$ and $y_{t+1} = Y_{t+1} - F$, we can rewrite the system more conveniently as Eq. (21) in Box II Note that map B exhibits the same dynamics as map A, except that its variables are expressed on deviations from the oil market's fundamental value.

The state space is partitioned into four regions, say $\mathcal{B}_1$, $\mathcal{B}_2$, $\mathcal{B}_3$ and $\mathcal{B}_4$, as shown in Fig. 1.

In region $\mathcal{B}_1$, the oil market is significantly undervalued — specifically, the price deviation from the fundamental value falls below the threshold $-\frac{h}{d}$ — and speculators refrain from holding oil across two consecutive periods. Since their position in the oil market does not change, they neither buy nor sell oil, the market dynamics and the associated stability condition follow those of the linear cobweb model without speculators. However, as established in Proposition 1, no equilibria exist in region $\mathcal{B}_1$.

In region $\mathcal{B}_2$, speculators liquidate all oil stocks held from the previous period, effectively acting as suppliers in the market. This additional supply results in a lower market price than would prevail in a cobweb model without speculators. The linear map governing this region admits an equilibrium at $\bar{x} = \bar{y} = -\frac{h}{b+c+d}$. Relative to the standard cobweb model, the condition for equilibrium stability is relaxed with respect to parameter c: stability requires $c < b+d$, rather than the stricter condition $c < b$. However, an additional constraint must be met concerning the intensity of speculative trading — specifically, $d < b$.

In region $\mathcal{B}_3$, speculators replenish oil stocks that were depleted in the previous period for speculative purposes. As buyers in the market, their demand pushes the price above the level observed in a cobweb market without speculators. The linear map governing this region admits an equilibrium at $\bar{x} = \bar{y} = \frac{h}{b+c-d}$. Compared to the cobweb model without speculators, the stability condition is relaxed with respect to the upper bound on parameter c: specifically, stability requires $c < b+d$, rather than the more restrictive $c < b$. However, when $d > b$, stability also requires a lower bound on c: namely, $c > d - b$. This implies that a higher value of the speculator reaction parameter d enhances stability as long as $d < b$, in which case the market is more stable than under standard cobweb dynamics. Conversely, if $d > b$, the additional lower bound condition on c becomes necessary to maintain stability.

Finally, consider region $\mathcal{B}_4$. Economically, this scenario corresponds to a situation in which, for two consecutive periods, the oil market avoids being substantially undervalued — that is, the price does not fall below its fundamental value by more than $-\frac{h}{d}$. In this context, speculators hold oil across both periods. However, their stock levels may vary, and their net demand for oil in each period can be either positive or negative. As a result, the market price may differ from that observed in a cobweb market without speculators. In period $t+1$, this difference is quantified by $\frac{d}{b}(x_t - y_t)$, which is positive when prices are increasing over the last two periods. In region $\mathcal{B}_4$, there exists a real steady state at $\bar{x} = \bar{y} = 0$, which is locally stable provided that $c < b+2d$ and $d < b$. Compared to the cobweb market without speculators, the condition for stability is less restrictive on the upper bound of parameter c: specifically, it requires $c < b + 2d$ instead of the more

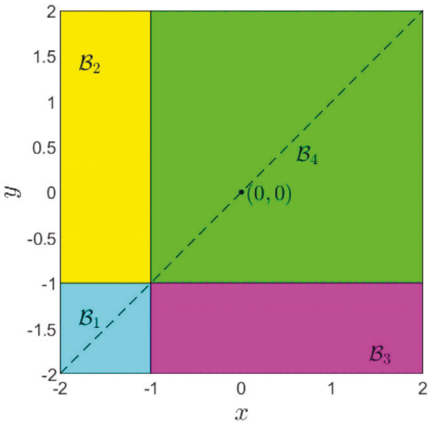

Fig. 1. State space of map B partitioned in the subregions $\mathcal{B}_1$ (cyan), $\mathcal{B}_2$ (yellow), $\mathcal{B}_3$ (magenta) and $\mathcal{B}_4$ (green). Parameters: $b = 1$ and $h = 1$.

stringent $c < b$. However, an additional condition must be imposed on parameter d, which governs the order size of speculators — namely, $d < b$. Therefore, as long as speculators are not overly active (i.e., $d < b$), the stability region is expanded relative to that of a cobweb market without speculators.

We summarize the main properties of the dynamics of map B in the following proposition (the proof of which is in Appendix A).

Proposition 1. *The map B, where parameters b, c, d and h are positive, is such that:*

(1) If an equilibrium exists, it lies along the diagonal $x = y$, and therefore must be located either in region $\mathcal{B}_1$ or in region $\mathcal{B}_4$;
(2) Region $\mathcal{B}_1$ is mapped into the line spanned by the vector $[-c/b, 1]$, that is the line of equation $y = -(b/c)\,x$;
(3) Region $\mathcal{B}_3$ is mapped into the line of equation $y = (bx - h)/(d - c)$;
(4) The map that applies in $\mathcal{B}_1$ has equilibrium $(0,0) \notin \mathcal{B}_1$, which is locally stable for $0 \le c < b$.
(5) The map that applies in $\mathcal{B}_2$ has equilibrium $\left(-\frac{h}{b+c+d}, -\frac{h}{b+c+d}\right) \notin \mathcal{B}_2$, which is locally stable for $0 \le c < b + d$ and $d < b$;
(6) The map that applies in $\mathcal{B}_3$ has equilibrium $\left(\frac{h}{b+c-d}, \frac{h}{b+c-d}\right) \notin \mathcal{B}_3$, which is locally stable for $\max\{0; d - b\} < c < d + b$.
(7) The map that applies in $\mathcal{B}_4$ has equilibrium $(0,0) \in \mathcal{B}_4$, which is locally stable for $b > d$ and $0 \le c < b + 2d$;
(8) The map B has a unique real equilibrium $(0,0)$, which is locally stable for $b > d$ and $0 \le c < b + 2d$;

2.2. Some further insights

Fig. 2 shows two two-dimensional (2D) bifurcation diagrams for map B, setting $b = 1$ and $h = 1$. In the left panel, initial conditions are close to the origin whereas they are more distant in the right panel. The parameter space is color-coded to indicate the long-term behavior associated with the chosen initial conditions: yellow indicates convergence to the fundamental equilibrium; red, cyan, green, and blue correspond to period-three, -four, -five, and -six cycles, respectively; other colors represent higher-period cycles up to period fourteen; white indicates cycles of period higher than fourteen or chaotic dynamics; and gray denotes unbounded behavior. Recall that the model without speculators produces fixed-point dynamics for $c < b$ and divergent dynamics for $c > b$. Obviously, speculators have a non-trivial impact on the dynamics of the oil market. For $c < b$ as well as for $c > b$, we may observe fixed-point dynamics, bounded dynamics, or divergent dynamics. However, it is also clear that speculators prevent fixed-point dynamics for $d > 1$, irrespective of the relationship between parameters c and b. By increasing the tax rate τ, policymakers decrease parameter c, and there is a tendency, but not a guarantee, that the oil market will display fixed-point or bounded dynamics. Apart from that, it is clear that when the oil price converges to its fundamental value (yellow parameter space), the same policy implications apply as in the traditional cobweb model: higher tax rates increase the fundamental value of the oil price and reduce steady-state oil consumption.

An overview of the possible endogenous oil price dynamics generated by the model is provided through a set of exploratory examples. In all cases, we set $b = 1$ and $h = 1$, and vary the parameters c and d. In the first example, we fix $c = 1.15 > 1$ and $d = 1.4 > 1$. Under these parameter values, the standard cobweb model exhibits divergent behavior. By contrast, our oil market model with speculators generates irregular, complex dynamics. The trajectory in the state space is shown in the left panel of Fig. 3, this trajectory depicts an invariant chaotic set as discussed in Appendix B, while the corresponding time series of the price deviation from the fundamental price, say x, is displayed in the right panel. This example confirms that speculators play a dual role: on one hand, they help stabilize the market by taking speculative long positions when the market price falls below the fundamental value, thereby offsetting excess supply and preventing unbounded divergence; on the other hand, their trading behavior also contributes to oil market volatility.

In the second example, we fix $c = 1.35 > 1$ and $d = 0.99 < 1$. Under these parameter values, the model without speculators exhibits divergent dynamics. In contrast, the model with speculators admits a locally stable fundamental equilibrium that coexists with a period-three cycle. The trajectory along the period-three cycle in the state space is shown in the left panel of Fig. 4, with the fixed point depicted in red. The basins of attraction of the fixed point and the period-three cycle are shown in yellow and magenta, respectively. The corresponding time series of the price deviation from the fundamental value is displayed in the right panel of Fig. 4. Once again, speculators help prevent unbounded price divergence by taking speculative long (short) positions during periods of oversupply (undersupply) by producers, though two side effects arise. First, there is an increased risk of excessive volatility. Second, as discussed in more detail in Section 4, exogenous shocks may trigger regime-switching dynamics, pushing the system back and forth between the basins of attraction of the fundamental equilibrium and the period-three cycle, thereby generating volatility outbursts, a phenomenon frequently observed in actual oil markets.

Chaos can emerge even in an oil market where, in the absence of speculators, the fundamental equilibrium would be globally stable. We illustrate this with two examples, while Appendix B demonstrates that these dynamics are indeed chaotic.

In the first case (the third example), we set $c = 0.7 < 1$ and $d = 1.1 > 1$. Under these conditions, the system exhibits a unique attractor, which is chaotic. The dynamics in the state space are shown in the left panel of Fig. 5, while the time series of the price deviation from the fundamental value (i.e., x) is displayed in the right panel.

In the second case (the fourth example), we set $c = 0.55 < 1$ and $d = 1.25 > 1$. Despite the lower value of c, which would typically enhance stability, we still observe a unique chaotic attractor. The dynamics in the state space are shown in the left panel of Fig. 6, and the corresponding time series of x is displayed in the right panel.

In a fifth example, we set $c = 0.05 < 1$ and $d = 1.2 > 1$. These parameter values describe an oil market dominated by speculators, who destabilize an otherwise stable fundamental equilibrium. In contrast, a high cost of production, a high taxation rate, or a combination of both tends to minimize the influence of suppliers on the market dynamics. As a result, a stable period-six cycle emerges. The dynamics in the state space are shown in the left panel of Fig. 7, while the time series of the price deviation from the fundamental value (i.e, x) is displayed in the right panel.

A further interesting example (sixth example) arises when we set $c = 0.65 < 1$ and $d = 1.5 > 1$. In the case of a cobweb oil market model

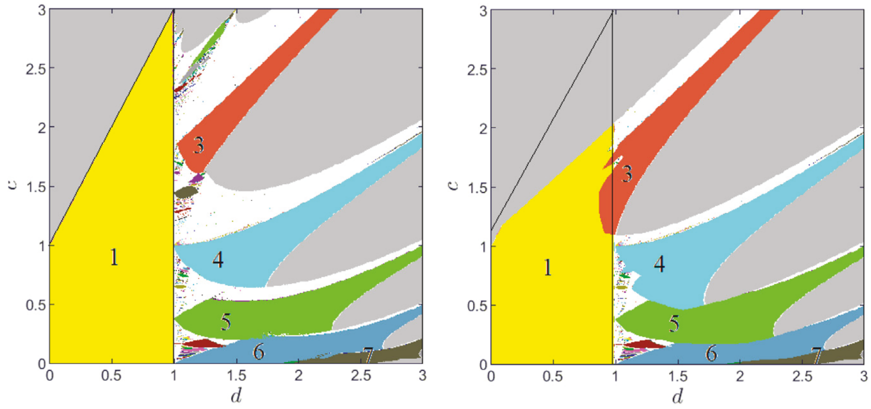

Fig. 2. Two-dimensional bifurcation diagrams for map B, using $b = 1$ and $h = 1$. Left: Initial conditions close to origin. Right: Initial conditions distant to origin. (For interpretation of the references to color in this figure legend, the reader is referred to the web version of this article.)

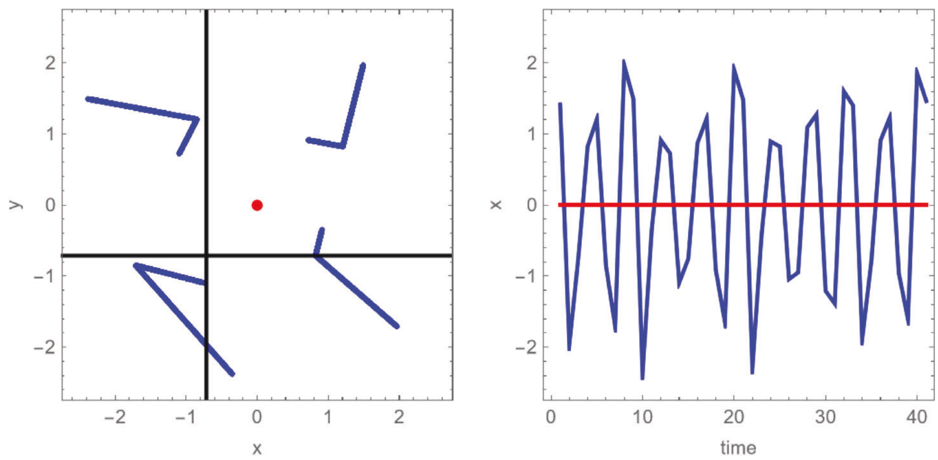

Fig. 3. Example 1. Left panel: The chaotic attractor is shown in blue, while the fundamental equilibrium is depicted in red. Right panel: Time series of the state variable x along the chaotic attractor (blue) and the fundamental equilibrium (red). Parameters: $b = 1$, $c = 1.15$, $d = 1.4$, and $h = 1$. (For interpretation of the references to color in this figure legend, the reader is referred to the web version of this article.)

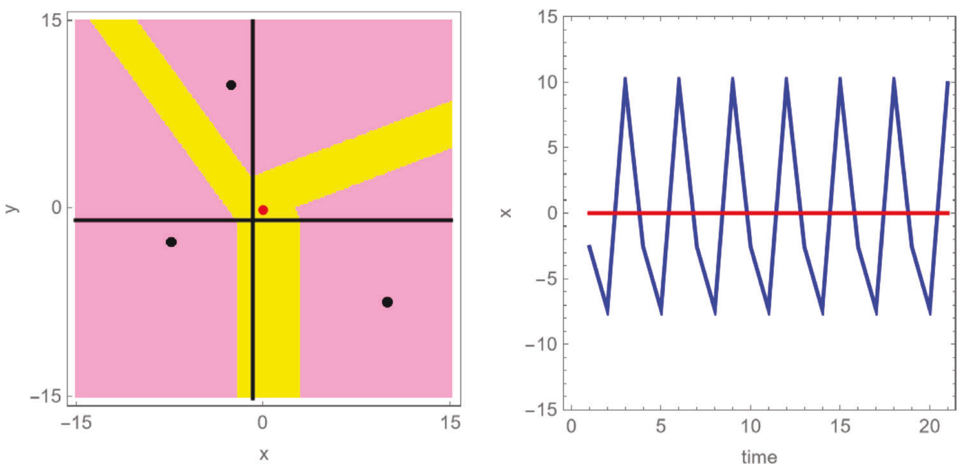

Fig. 4. Example 2. Left panel: The period-three cycle in shown in black (in magenta its basin of attraction) and the fundamental equilibrium in red (in yellow its basin of attraction). Right panel: Time series of the state variable x along the period-three cycle (blue) and the fundamental equilibrium (red). Parameters: $b = 1$, $c = 1.35$, $d = 0.99$, and $h = 1$. (For interpretation of the references to color in this figure legend, the reader is referred to the web version of this article.)

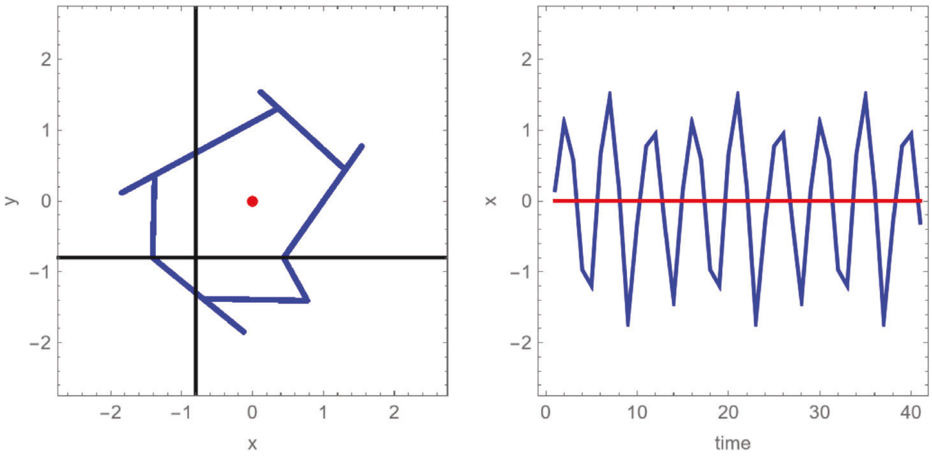

Fig. 5. Example 3. Left panel: The chaotic attractor is shown in blue (in white its basin of attraction), while the fundamental equilibrium is depicted in red. Right panel: Time series of the state variable x along the chaotic attractor (blue) and the fundamental equilibrium (red). Parameters: $b = 1$, $c = 0.55$, $d = 1.25$, and $h = 1$. (For interpretation of the references to color in this figure legend, the reader is referred to the web version of this article.)

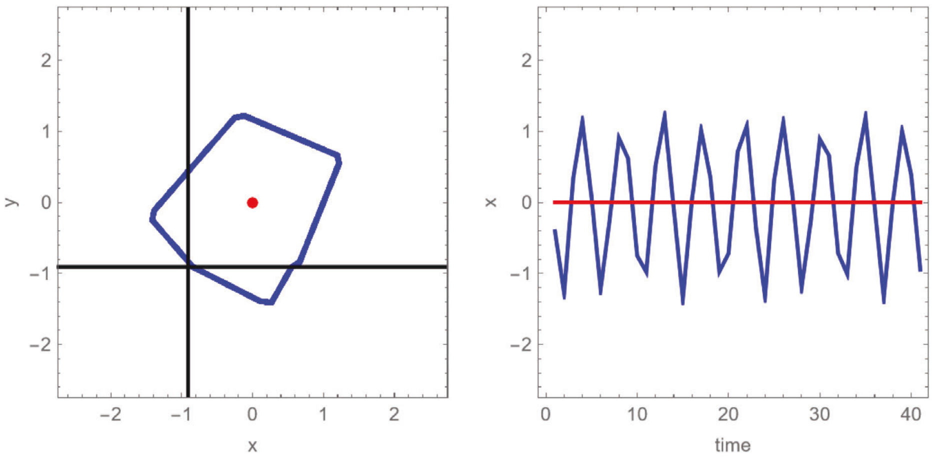

Fig. 6. Example 4. Left panel: The chaotic attractor is shown in blue, while the fundamental equilibrium is depicted in red. Right panel: Time series of the state variable x along the chaotic attractor (blue) and the fundamental equilibrium (red). Parameters: $b = 1$, $c = 0.7$, $d = 1.1$, and $h = 1$. (For interpretation of the references to color in this figure legend, the reader is referred to the web version of this article.)

without speculators (i.e., $d = 0$), the fundamental equilibrium would be stable. However, the presence of speculators in this setting destabilizes the fundamental equilibrium, illustrating how speculative behavior can serve as a source of endogenous instability. Even more noteworthy is the nature of the resulting dynamics: a stable period-four cycle coexists with a chaotic attractor, highlighting the potential for complex regime-switching behavior depending on initial conditions. These two attractors are depicted in the state space in Fig. 8, along with their respective basins of attraction. Their structure reveals indeed a high sensitivity to initial conditions, with a complex boundary separating the basins — suggesting the possibility of abrupt transitions between the periodic and chaotic regimes. The time series of the price deviation from the fundamental value (i.e., x) is shown in the right panel of Fig. 8.

The seventh example illustrates the coexistence of stable periodic cycles. We set $c = 0.52 < 1$ and $d = 1.5 > 1$. In the corresponding cobweb oil market model without speculators (i.e., $d = 0$), the fundamental equilibrium would be stable. However, as in the previous example, the introduction of speculators destabilizes the fundamental equilibrium. Unlike the previous case, the resulting dynamics do not exhibit chaos: instead, a stable period-four cycle coexists with a stable period-five cycle. These two attractors are shown in the state space in Fig. 9, along with their respective basins of attraction.

Finally, we conduct a sensitivity analysis with respect to two key model parameters. The left panel of Fig. 10 presents a one-dimensional bifurcation diagram for map B, in which the oil price (measured as deviations from its fundamental value) is plotted against the inverse tax-adjusted cost parameter c, while holding the remaining parameters fixed at $b = 1$, $d = 1.2$, and $h = 1$. As c increases from 0 to 1.6, the system exhibits a sequence of periodic and chaotic attractors, implying discontinuous regime shifts and sudden qualitative changes in the oil price dynamics rather than gradual adjustments. The right panel displays a bifurcation diagram obtained by fixing $b = 1$, $c = 0.2$, and $h = 1$, and varying the risk-adjusted expectation parameter d between 0.95 and 1.85. For $d < 1$, the oil price converges to its fundamental value. Once d exceeds the critical threshold $d = 1$, endogenous price fluctuations with a significant amplitude emerge immediately. As d increases further, the amplitude of these fluctuations tends to increase.

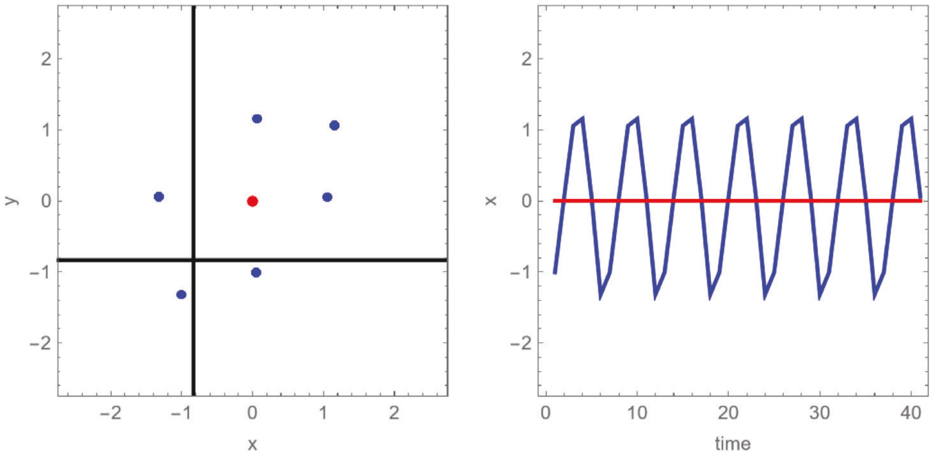

Fig. 7. Example 5. Left panel: The period-six cycle is shown in blue, while the fundamental equilibrium is depicted in red. Right panel: Time series of the state variable x along the period-six cycle (blue) and the fundamental equilibrium (red). Parameters: $b = 1$, $c = 0.05$, $d = 1.2$, and $h = 1$. (For interpretation of the references to color in this figure legend, the reader is referred to the web version of this article.)

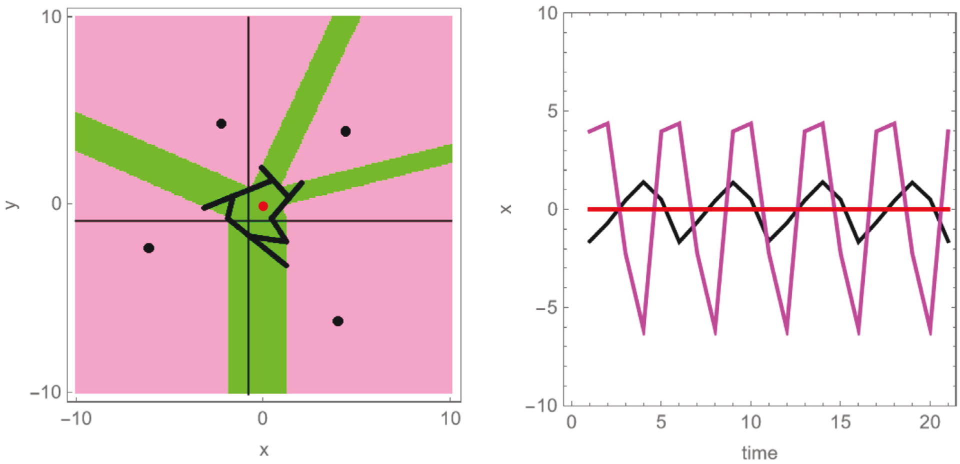

Fig. 8. Example 6. Left panel: The period-four cycle is shown in black (its basin of attraction is in magenta), the chaotic attractor is also shown in black (its basin of attraction is in green), while the fundamental equilibrium is depicted in red. Right panel: Time series of the state variable x along the period-four cycle (in magenta), along the chaotic attractor (black) and the fundamental equilibrium (red). Parameters: $b = 1$, $c = 0.65$, $d = 1.5$, and $h = 1$.

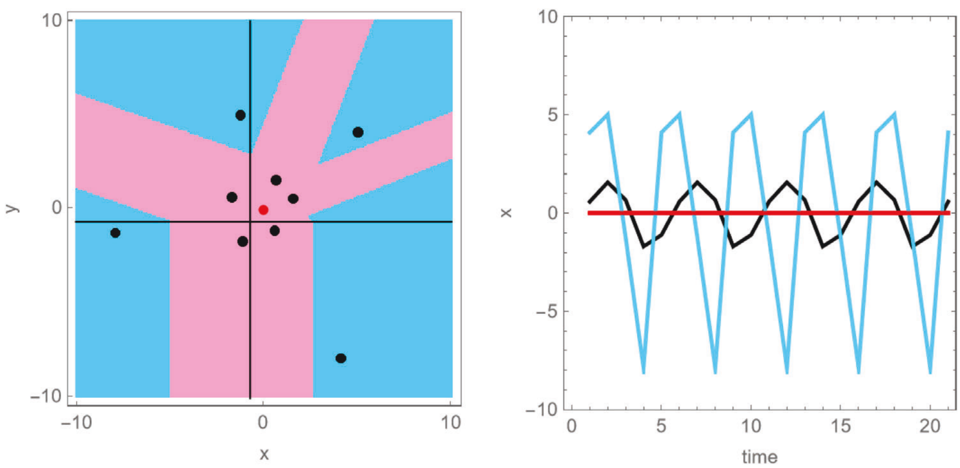

Fig. 9. Example 7. Left panel: The period-five cycle is shown in black (in cyan its basin of attraction), the period-five cycle in black (in magenta its basin of attraction), and the fundamental equilibrium in red. Right panel: Time series of the state variable x along the period-four cycle (in cyan) and along the period-five cycle (in black). Parameters: $b = 1$, $c = 0.52$, $d = 1.5$, and $h = 1$.

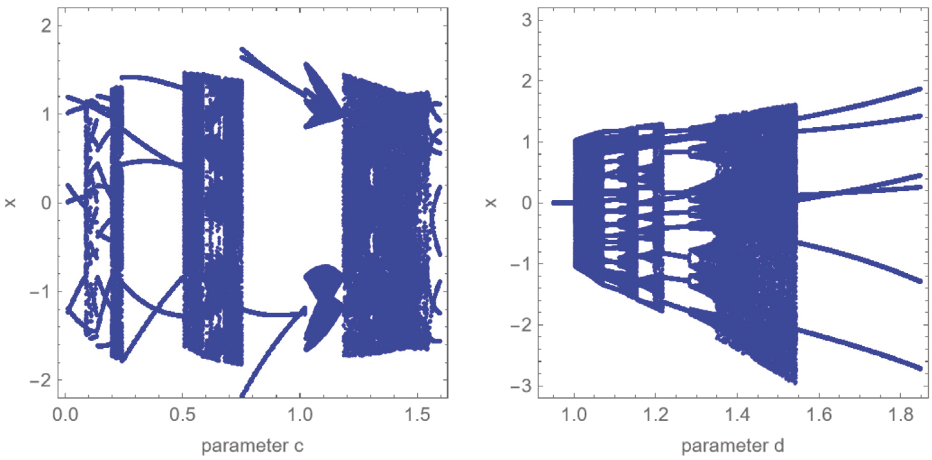

Fig. 10. One-dimensional bifurcation diagrams for map B. Left panel: $b = 1$, $0 < c < 1.6$, $d = 1.2$, and $h = 1$. Right panel: $b = 1$, $c = 0.2$, $0.95 < d < 1.85$, and $h = 1$.

3. Extensions and robustness checks

In this section, we present several model extensions and robustness checks.

3.1. An upper storage limit

Let us first consider that speculators' position in the oil market cannot be negative nor exceed an upper storage limit. For ease of exposition, let us furthermore assume that the upper storage limit is twice the long-run portfolio position in the oil market. Thus, speculators desired position in the oil market is

$$\delta_{t+1} = \begin{cases} 2h & \text{if} \quad h + d\left(P_t - F\right) > 2h \\ h + d\left(P_t - F\right) & \text{if} \quad 0 \leq h + d\left(P_t - F\right) \leq 2h \\ 0 & \text{if} \quad h + d\left(P_t - F\right) < 0 \end{cases} . \tag{22}$$

Now there are three generic scenarios, and the economic meaning of the switching boundaries is as follows. If speculators are very pessimistic about the future oil price, their position in the market is zero, as they have sold all oil held in storage. If speculators are very optimistic about the future oil price, their position in the market is given by $2h$, and they have bought as much oil as they can store. For moderate degrees of optimism and pessimism, speculators' position lies between these two extremes. They hold more oil than warranted by their long-run portfolio position when they are mildly optimistic and less oil than warranted by their long-run portfolio position when they are mildly pessimistic. Clearly, their position always remains within their storage capacity. When the oil price equals its fundamental value, speculators' position (denoted by δ_t for any time t) equals h.

Since δ_{t+1} is now piecewise defined with three branches, the relation $\Delta_{t+1} = \delta_{t+1} - \delta_t$ yields a total of nine cases, and the dynamics of our extended oil market model is governed by the two-dimensional piecewise linear map (see the Eq. (23) in Box III): where $Y_{t+1} = P_t$ is again an auxiliary variable. Using $x_{t+1} = P_{t+1} - F$ and $y_{t+1} = Y_{t+1} - F$, we obtain (see the Eq. (24) in Box IV)

Note that map D exhibits the same dynamics as map C, except that its variables are expressed on deviations from the oil market's fundamental value. The state space is partitioned into nine regions, say $\mathcal{D}_1, \ldots, \mathcal{D}_9$, as shown in Fig. 11.

The observations made for map B in regions $\mathcal{B}1$, $\mathcal{B}2$, $\mathcal{B}3$, and $\mathcal{B}4$ also apply to map D in regions $\mathcal{D}1$, $\mathcal{D}2$, $\mathcal{D}4$, and $\mathcal{D}5$, respectively.

Regarding region $\mathcal{D}_3$, note that $\mathcal{D}_2 \cup \mathcal{D}_3 = \mathcal{B}_2$. In region $\mathcal{D}_2$, the dynamics under map D mirror those under map B: speculators fully liquidate the oil stocks accumulated in the previous period, effectively acting as suppliers. This additional supply pushes the market price

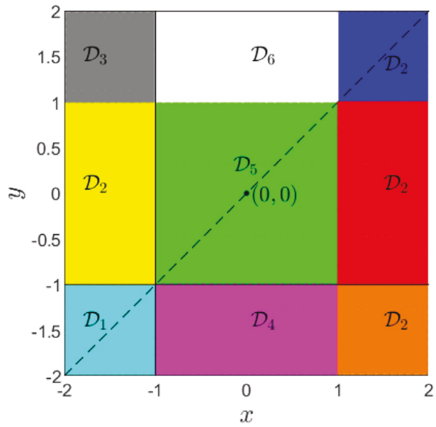

Fig. 11. State space of map D partitioned in the subregions $\mathcal{D}_1$ (cyan), $\mathcal{D}_2$ (yellow), $\mathcal{D}_3$ (gray), $\mathcal{D}_4$ (magenta), $\mathcal{D}_5$ (green), $\mathcal{D}_6$ (white), $\mathcal{D}_7$ (orange), $\mathcal{D}_8$ (red) and $\mathcal{D}_9$ (blue). Parameters: $b = 1$ and $h = 1$. (For interpretation of the references to color in this figure legend, the reader is referred to the web version of this article.)

lower than in a standard cobweb model without speculators, thereby relaxing the stability conditions for the fundamental equilibrium. A similar effect occurs in region $\mathcal{D}_3$, although it is mitigated under map D because the quantity of oil liquidated is smaller — limited by the active maximum capacity constraints in the preceding period.

Region $\mathcal{D}_6$, as with region $\mathcal{B}_4$ under map B, corresponds to a situation in which, for two consecutive periods, the oil market avoids being substantially undervalued — that is, the price does not fall below its fundamental value by more than $-\frac{h}{d}$. In this context, speculators hold oil across both periods. However, their stock levels decline in the final period, as $y_t > x_t$ in $\mathcal{D}_6$, indicating falling prices. Consequently, speculators' net demand for oil becomes negative in the last period, although it is less negative than it would be in the absence of maximum capacity constraints. This mitigates the potential for an excessive price drop and contributes to a relaxation of the stability conditions.

Region $\mathcal{D}_7$, as with region $\mathcal{B}_4$ under map B, corresponds to a situation in which in the last period the oil price was overpriced, that is its price was above the threshold $\frac{h}{d}$. Speculators' position have turned positive after previously being negative, so the net extra demand is high, though still lower than it would be under map B due to the imposed constraint. This limitation of oversuply contributes to relax the stability conditions for the system that apply in this region.

$$C : \begin{cases} P_{t+1} &= \begin{cases} \frac{a}{b} - \frac{c}{b} P_t & \text{if} \quad P_t - F < -\frac{h}{d} \wedge Y_t - F < -\frac{h}{d} \\ \frac{a}{b} - \frac{h}{b} + \frac{d}{b} F - \frac{c}{b} P_t - \frac{d}{b} Y_t & \text{if} \quad P_t - F < -\frac{h}{d} \wedge -\frac{h}{d} \leq Y_t - F \leq \frac{h}{d} \\ \frac{a}{b} - \frac{2h}{b} - \frac{c}{b} P_t & \text{if} \quad P_t - F < -\frac{h}{d} \wedge Y_t - F > \frac{h}{d} \\ \frac{a}{b} + \frac{h}{b} - \frac{d}{b} F - \frac{c-d}{b} P_t & \text{if} \quad -\frac{h}{d} \leq P_t - F \leq \frac{h}{d} \wedge Y_t - F < -\frac{h}{d} \\ \frac{a}{b} - \frac{c-d}{b} P_t - \frac{d}{b} Y_t & \text{if} \quad -\frac{h}{d} \leq P_t - F \leq \frac{h}{d} \wedge -\frac{h}{d} \leq Y_t - F \leq \frac{h}{d} \\ \frac{a}{b} - \frac{h}{b} - \frac{d}{b} F - \frac{c-d}{b} P_t & \text{if} \quad -\frac{h}{d} \leq P_t - F \leq \frac{h}{d} \wedge Y_t - F > \frac{h}{d} \\ \frac{a}{b} + \frac{2h}{b} - \frac{c}{b} P_t & \text{if} \quad P_t - F > \frac{h}{d} \wedge Y_t - F < -\frac{h}{d} \\ \frac{a}{b} + \frac{h}{b} + \frac{d}{b} F - \frac{c}{b} P_t - \frac{d}{b} Y_t & \text{if} \quad P_t - F > \frac{h}{d} \wedge -\frac{h}{d} \leq Y_t - F \leq \frac{h}{d} \\ \frac{a}{b} - \frac{c}{b} P_t & \text{if} \quad P_t - F > \frac{h}{d} \wedge Y_t - F > \frac{h}{d} \end{cases} \\ Y_{t+1} &= P_t \end{cases}, \tag{23}$$

Box III.

$$D : \begin{cases} x_{t+1} &= \begin{cases} -\frac{c}{b} x_t & \text{if} \quad (x_t, y_t) \in \mathcal{D}_1 := \left\{ (x_t, y_t) \middle| x_t < -\frac{h}{d} \wedge y_t < -\frac{h}{d} \right\} \\ -\frac{c}{b} x_t - \frac{d}{b} y_t - \frac{h}{b} & \text{if} \quad (x_t, y_t) \in \mathcal{D}_2 := \left\{ (x_t, y_t) \middle| x_t < -\frac{h}{d} \wedge -\frac{h}{d} \leq y_t \leq \frac{h}{d} \right\} \\ -\frac{c}{b} x_t - \frac{2h}{b} & \text{if} \quad (x_t, y_t) \in \mathcal{D}_3 := \left\{ (x_t, y_t) \middle| x_t < -\frac{h}{d} \wedge y_t > \frac{h}{d} \right\} \\ -\frac{c-d}{b} x_t + \frac{h}{b} & \text{if} \quad (x_t, y_t) \in \mathcal{D}_4 := \left\{ (x_t, y_t) \middle| -\frac{h}{d} \leq x_t \leq \frac{h}{d} \wedge y_t < -\frac{h}{d} \right\} \\ -\frac{c-d}{b} x_t - \frac{d}{b} y_t & \text{if} \quad (x_t, y_t) \in \mathcal{D}_5 := \left\{ (x_t, y_t) \middle| -\frac{h}{d} \leq x_t \leq \frac{h}{d} \wedge -\frac{h}{d} \leq y_t \leq \frac{h}{d} \right\} \\ -\frac{c-d}{b} x_t - \frac{h}{b} & \text{if} \quad (x_t, y_t) \in \mathcal{D}_6 := \left\{ (x_t, y_t) \middle| -\frac{h}{d} \leq x_t \leq \frac{h}{d} \wedge y_t > \frac{h}{d} \right\} \\ -\frac{c}{b} x_t + \frac{2h}{b} & \text{if} \quad (x_t, y_t) \in \mathcal{D}_7 := \left\{ (x_t, y_t) \middle| x_t > \frac{h}{d} \wedge y_t < -\frac{h}{d} \right\} \\ -\frac{c}{b} x_t - \frac{d}{b} y_t + \frac{h}{b} & \text{if} \quad (x_t, y_t) \in \mathcal{D}_8 := \left\{ (x_t, y_t) \middle| x_t > \frac{h}{d} \wedge -\frac{h}{d} \leq y_t \leq \frac{h}{d} \right\} \\ -\frac{c}{b} x_t & \text{if} \quad (x_t, y_t) \in \mathcal{D}_9 := \left\{ (x_t, y_t) \middle| x_t > \frac{h}{d} \wedge y_t > \frac{h}{d} \right\} \end{cases} \\ y_{t+1} &= x_t \end{cases}. \tag{24}$$

Box IV.

Region $\mathcal{D}_7$, like region $\mathcal{B}_4$ under map B, represents a scenario where the oil price in the previous period was overpriced — that is, it exceeded the threshold $\frac{h}{d}$. In this region, speculators have shifted from negative to positive positions, resulting in a high net increase in demand. However, due to the constraints in place, this increase is smaller than it would be under map B. The resulting limitation on oversupply helps to ease the stability conditions that govern the system in this region.

Region $\mathcal{D}_8$ describes a situation where the most recent oil price exceeds the threshold $\frac{h}{d}$, while the price in the previous period was below it. Consequently, the net demand from speculators is positive but lower than it would be under map B in the same region, as capacity constraints limit speculative activity. This reduction in speculative pressure helps to stabilize the system.

Finally, in region $\mathcal{D}_9$, the oil price has been above the threshold $\frac{h}{d}$ — that is, overpriced — for the past two periods. As a result, speculators have already reached their maximum holding capacity and are no longer active in the market. Consequently, the market dynamics revert to those of the standard cobweb model, and the destabilizing influence of speculators is eliminated.

We summarize the main properties of the dynamics of map D in the following proposition (the proof of which is in Appendix A).

Proposition 2. *The map D, where parameters b, c, d and h are positive, has a unique (real) fixed point $(0, 0)$ at which the oil price is at its fundamental value. It is locally asymptotically stable, provided that $c < b + 2d$ and $d < b$.*

In summary, maximum capacity constraints do not affect the stability of the fundamental equilibrium. However, they are expected to limit speculative behavior during periods of extremely high oil prices. Since it is the net positions of speculators that influence the market, this effect may not always be clearly observable across all parameter configurations. This is illustrated by the 2D bifurcation diagrams in Fig. 12. This 2D bifurcation diagram shows that outside the stability region of the fundamental equilibrium, even for map D, as it is for map B, stable cycles of a different periodicity can emerge, along with chaotic dynamics. This confirms the robustness of our results.

We also conduct a sensitivity analysis for map D, keeping the parameter constellations and axis scaling identical to those used in Fig. 10 to facilitate comparison. The left panel of Fig. 13 presents a one-dimensional bifurcation diagram in which the oil price (measured as deviations from its fundamental value) is plotted against the inverse tax-adjusted cost parameter c, while holding the remaining parameters fixed at $b = 1$, $d = 1.2$, and $h = 1$. As c increases from 0 to 1.6, the system again exhibits a sequence of periodic and chaotic attractors, implying discontinuous regime shifts and sudden qualitative changes in the oil price dynamics. However, due to the upper storage constraint, the attractors are now symmetric around the origin, and the amplitude of price fluctuations is generally reduced. The right panel displays a

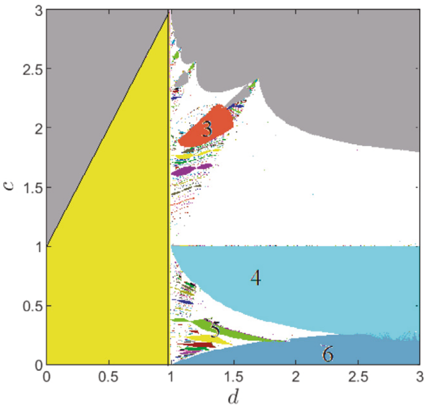

Fig. 12. Two-dimensional bifurcation diagram for map D, using $b = 1$ and $h = 1$. The significance of the colored regions in this figure is the same as in Fig. 2. (For interpretation of the references to color in this figure legend, the reader is referred to the web version of this article.)

bifurcation diagram obtained by fixing $b = 1$, $c = 0.2$, and $h = 1$, and varying the risk-adjusted expectation parameter d between 0.95 and 1.85. For $d < 1$, the oil price converges to its fundamental value. Once d exceeds the critical threshold $d = 1$, endogenous price fluctuations emerge immediately. Compared to map B, these fluctuations remain more symmetric and exhibit a smaller amplitude, although their magnitude still tends to increase as d rises further.

3.2. Price dynamics of structural model extensions

In this section, we illustrate the oil price dynamics generated by four structural model extensions. Each extension defines a distinct nonlinear dynamical system and may therefore warrant a comprehensive mathematical investigation in its own right. However, rather than providing a full analytical treatment, our objective here is more modest: we demonstrate by means of simulations that all four structural extensions are capable of generating endogenous oil price fluctuations. The price dynamics of each model extension are obtained by simulating the corresponding system of core economic equations. We begin with the first structural model extension, namely the introduction of an upper storage limit, which was formally developed and analyzed in Section 3.1. The market-clearing condition implies the oil price dynamics

$$P_{t+1} = \frac{a}{b} - \frac{S_{t+1}}{b} + \frac{\Delta_{t+1}}{b}. \tag{25}$$

Producers' oil supply is given by

$$S_{t+1} = cE_{o,t}\left[P_{t+1}\right], \tag{26}$$

where expectations are formed according to a naïve rule,

$$E_{o,t}\left[P_{t+1}\right] = P_t. \tag{27}$$

Speculators' demand or supply of oil is given by

$$\Delta_{t+1} = \delta_{t+1} - \delta_t. \tag{28}$$

Their desired position in the oil market is

$$\delta_{t+1} = \begin{cases} 2h & \text{if} \quad h + \frac{1}{\alpha}E_{s,t}\left[P_{t+2} - P_{t+1}\right] > 2h \\ h + \frac{1}{\alpha}E_{s,t}\left[P_{t+2} - P_{t+1}\right] & \text{if} \quad 2h \geq h + \frac{1}{\alpha}E_{s,t}\left[P_{t+2} - P_{t+1}\right] \geq 0 \\ 0 & \text{if} \quad 0 > h + \frac{1}{\alpha}E_{s,t}\left[P_{t+2} - P_{t+1}\right] \end{cases} \tag{29}$$

with expected price changes given by

$$E_{s,t}\left[P_{t+2} - P_{t+1}\right] = \beta\left(P_t - F\right) \tag{30}$$

and aggregate parameter $d = \frac{\beta}{\alpha}$. The top-left panel of Fig. 14 displays a simulation run for the parameter constellation $a = 10$, $b = 1$, $c = 1.25$, $d = 1.85$, and $h = 1$. The oil price exhibits persistent endogenous oscillations around its fundamental value.

As an additional model extension, suppose that producers face larger production lags. This can be implemented by replacing the naïve expectation rule with the adaptive scheme

$$\tilde{E}_{o,t}\left[P_{t+1}\right] = \tau P_t + (1-\tau)\,\tilde{E}_{o,t-1}\left[P_t\right] \tag{31}$$

with $0 < \tau < 1$. Under this rule, producers no longer fully adjust their expectations to the most recent price observation. Instead, expected prices are formed as a weighted average of the current price and previously held expectations. The parameter τ governs the speed of adjustment: the smaller τ, the more strongly expectations are anchored in the past and the more sluggishly they react to new information. Economically, this mechanism captures larger production lags, since supply decisions respond only gradually to current price signals.[8] The top-right panel of Fig. 14 shows a corresponding simulation run based on $a = 10$, $b = 1$, $c = 1.25$, $d = 1.85$, $h = 1$, and $\tau = 0.25$. The oil price again exhibits persistent endogenous fluctuations around its fundamental value.

So far, we have assumed that the upper storage limit is fixed. However, market participants may expand storage capacity when prices increase, for instance by renting additional facilities or investing in new infrastructure. To capture this idea, we allow the upper storage limit to depend positively on (expected) prices. Specifically, we assume

$$\delta_{t+1} = \begin{cases} 2h + \phi\tilde{E}_{o,t}[P_{t+1}] & \text{if } h + \frac{1}{\alpha}E_{s,t}[P_{t+2} - P_{t+1}] > 2h + \phi\tilde{E}_{o,t}[P_{t+1}], \\ h + \frac{1}{\alpha}E_{s,t}[P_{t+2} - P_{t+1}] & \text{if } 0 \leq h + \frac{1}{\alpha}E_{s,t}[P_{t+2} - P_{t+1}] \leq 2h + \phi\tilde{E}_{o,t}[P_{t+1}], \\ 0 & \text{if } h + \frac{1}{\alpha}E_{s,t}[P_{t+2} - P_{t+1}] < 0. \end{cases} \tag{32}$$

where ϕ measures the sensitivity of storage capacity to (expected) prices and $E_{s,t}[P_{t+2} - P_{t+1}]$ is defined as in (30). Under this specification, the effective upper storage limit increases when expected prices rise, while the lower limit remains fixed at zero. As a consequence, the symmetry of storage capacities around the reference level h is destroyed. This asymmetry is also reflected in the oil price dynamics. The bottom-left panel of Fig. 14, based on $a = 10$, $b = 1$, $c = 1.25$, $d = 1.85$, $h = 1$, $\tau = 0.25$, and $\phi = 0.08$, shows that oil price fluctuations become asymmetric with respect to the fundamental value.

Finally, we relax the assumption $\delta_{t+1} \geq 0$. We now allow speculators to take limited short positions by assuming

$$\delta_{t+1} = \begin{cases} 2h + \phi\tilde{E}_{o,t}[P_{t+1}] & \text{if } h + \frac{1}{\alpha}E_{s,t}[P_{t+2} - P_{t+1}] > 2h + \phi\tilde{E}_{o,t}[P_{t+1}], \\ h + \frac{1}{\alpha}E_{s,t}[P_{t+2} - P_{t+1}] & \text{if } -\epsilon \leq h + \frac{1}{\alpha}E_{s,t}[P_{t+2} - P_{t+1}] \leq 2h + \phi\tilde{E}_{o,t}[P_{t+1}], \\ -\epsilon & \text{if } h + \frac{1}{\alpha}E_{s,t}[P_{t+2} - P_{t+1}] < -\epsilon. \end{cases} \tag{33}$$

where $\epsilon > 0$ determines the maximum admissible short position. This specification increases overall storage flexibility by allowing speculative inventories to become negative within limits. The bottom-right panel of Fig. 14 presents a simulation run based on $a = 10$, $b = 1$, $c = 1.25$, $d = 1.85$, $h = 1$, $\tau = 0.25$, $\phi = 0.08$, and $\epsilon = 0.35$. Compared to the previous specification, the oil price exhibits more pronounced fluctuations around its fundamental value. Increasing storage flexibility thus appears to amplify price movements, as speculative positions can now adjust more strongly in both directions.

[8] This alternative expectation specification also reflects the fact that speculators and producers in the oil market adjust their positions at different speeds. While speculators can react almost immediately to new information, producers face adjustment lags due to production and investment constraints.

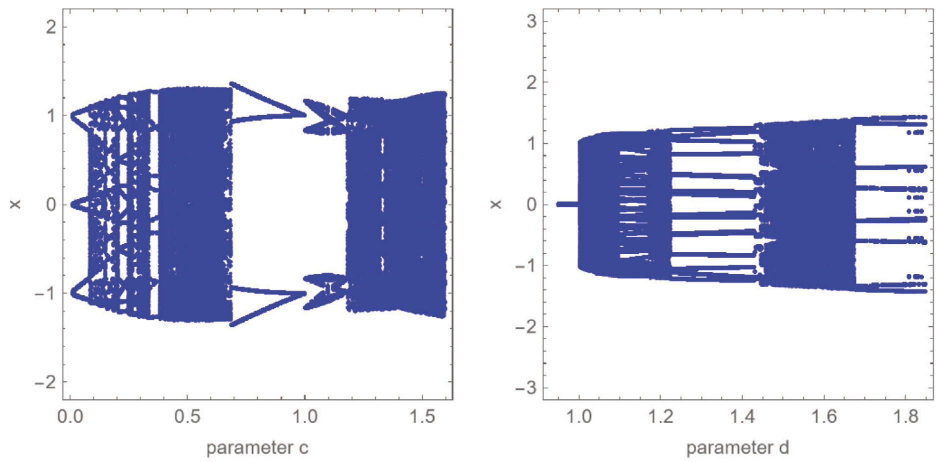

Fig. 13. One-dimensional bifurcation diagrams for map D. Left panel: $b = 1$, $0 < c < 1.6$, $d = 1.2$, and $h = 1$. Right panel: $b = 1$, $c = 0.2$, $0.95 < d < 1.85$, and $h = 1$.

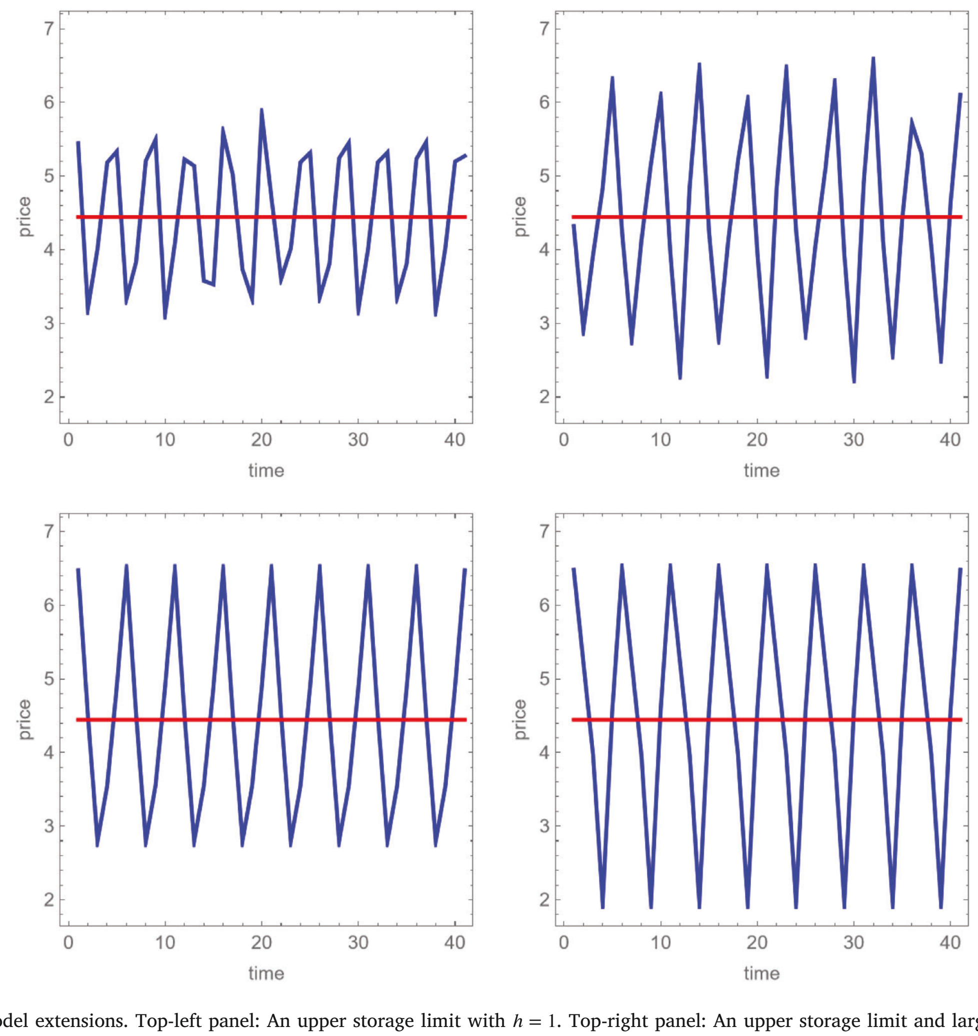

Fig. 14. Structural model extensions. Top-left panel: An upper storage limit with $h = 1$. Top-right panel: An upper storage limit and larger production lags with $h = 1$ and $\tau = 0.25$. Bottom-left panel: A price-dependent upper storage limit and larger production lags with $h = 1$, $\tau = 0.25$, and $\phi = 0.08$. Bottom-right panel: A price-dependent upper storage limit, a negative lower storage limit, and larger production lags with $h = 1$, $\tau = 0.25$, $\phi = 0.08$, and $\epsilon = 0.35$. Remaining parameters: $a = 10$, $b = 1$, $c = 1.25$, and $d = 1.85$.

3.3. Price dynamics of behavioral model extensions

So far, we have modeled speculators' expectations about future oil price changes by means of a simple extrapolative rule,

$$E_{s,t}\left[P_{t+2}-P_{t+1}\right]=E^{C}_{s,t}\left[P_{t+2}-P_{t+1}\right], \tag{34}$$

where

$$E^{C}_{s,t}\left[P_{t+2}-P_{t+1}\right]=\beta\left(P_t-F\right) \tag{35}$$

and $\beta>0$ denotes the extrapolation parameter. We now assume that speculators can switch between this extrapolative rule and a regressive rule, specified as

$$E^{R}_{s,t}\left[P_{t+2}-P_{t+1}\right]=e\left(F-P_t\right), \tag{36}$$

where $0<e<1$ measures the expected speed of mean reversion. The market share of speculators using the extrapolative rule is given by

$$W^{C}_{t}=\frac{1}{1+f\left(P_t-F\right)^2}, \tag{37}$$

where $f>0$ is a switching parameter. This formulation implies that the fraction of extrapolators decreases as the price deviates further from its fundamental value. Accordingly, when a bubble builds up in the oil market, more speculators adopt the regressive rule, expecting prices to return to fundamentals. Such a framework has been used by He and Westerhoff (2005) to model heterogeneous expectation formation in commodity markets. Speculators' average price change expectations are then given by

$$E_{s,t}\left[P_{t+2}-P_{t+1}\right]=W^{C}_{t}E^{C}_{s,t}\left[P_{t+2}-P_{t+1}\right]+\left(1-W^{C}_{t}\right)E^{R}_{s,t}\left[P_{t+2}-P_{t+1}\right]. \tag{38}$$

This specification introduces an additional source of nonlinearity into the oil market model via endogenous switching between forecasting strategies. The left panel of Fig. 15, based on $a=10$, $b=1$, $c=1.25$, $\beta=1.85$, $\alpha=1$ (implying $d=\frac{\beta}{\alpha}=1.85$), $e=0.25$, $f=0.1$, and $h=1$, shows that the model continues to generate endogenous oil price fluctuations when speculators exhibit boundedly rational learning behavior.

As a further behavioral model extension, we consider a genuinely trend-extrapolative forecasting rule,

$$E^{C}_{s,t}[P_{t+2}-P_{t+1}]=\beta\left(P_t-P_{t-1}\right), \tag{39}$$

where $\beta>0$ indicates the strength of trend extrapolation.

In this case, speculators switch between a trend-following rule and the regressive rule defined above. The right panel of Fig. 15, based on $a=10$, $b=1$, $c=1.25$, $\beta=1.05$, $\alpha=1$ (implying $d=\frac{\beta}{\alpha}=1.05$), $e=0.25$, $f=0.1$, and $h=1$, displays an example of the resulting oil price dynamics.

The model again produces persistent endogenous oil price fluctuations, demonstrating that such dynamics also arise when speculators switch between a truly trend-extrapolating rule and a regressive rule. Overall, these simulations suggest that the emergence of endogenous oil price dynamics is robust with respect to alternative expectation formation mechanisms.

A final behavioral model extension is to consider speculators' average price change expectations are then given by

$$E_{s,t}\left[P_{t+2}-P_{t+1}\right]=\beta\left(P_t-P_{t-1}\right). \tag{40}$$

A microfoundation for this extrapolative expectation rule is provided in Appendix D. There, it is shown that (40) is consistent with an infinite population of speculators holding a continuum of beliefs about future price deviations, distributed normally and updated according to a logit-choice rule.

Under this behavioral extension of the model, we continue to observe both periodic and chaotic dynamics; see the left and right panels of Fig. 16, respectively.

4. Empirical evidences and stochastic model dynamics

Thus far, our deterministic model has been shown to generate endogenous oil price fluctuations which, in a qualitative sense, can be interpreted as boom–bust dynamics. Given that the fundamental value is constant, these fluctuations also signal excess volatility. In this section, we provide a more detailed comparison of the dynamics of a stochastic extension of the oil market model presented in Section 2 with the observed behavior of actual oil prices. Section 4.1 reviews the historical evolution of empirically observed oil prices, while Section 4.2 introduces demand and supply shocks into the model in order to examine their effects on price dynamics. Section 4.3 provides a statistical comparison of actual and simulated oil prices.

4.1. Actual oil price dynamics

Fig. 17 illustrates the behavior of Brent crude oil prices (denominated in U.S. dollars per barrel), obtained from the FRED database of the Federal Reserve Bank of St. Louis.[9] The top panel displays the evolution of 9714 daily oil prices from May 20, 1987, to August 31, 2025, while the bottom panel shows the corresponding return dynamics. As is evident, oil prices exhibit pronounced boom–bust cycles and recurrent volatility outbursts, reflecting the impact of geopolitical shocks, macroeconomic cycles, and speculative forces. For more detailed historical accounts, see Kilian (2009), Cifarelli and Paladino (2010), Gong et al. (2020), Smales (2021), Harrison et al. (2023), and Zhang et al. (2024).

A brief review of this period shows the following. Between 1987 and 2000, oil prices generally fluctuated between \$15 and \$25 per barrel. During the Gulf War of 1990, however, prices surged to nearly \$40, while the Asian financial crisis of 1997–98 drove them below \$12. The early 2000s witnessed renewed growth, fueled by rising global oil consumption, culminating in a speculative surge to \$147 per barrel in 2008. Following the global financial crisis of 2008, prices collapsed to \$35 per barrel. A subsequent recovery sustained prices above \$90 between 2010 and 2014, but increasing oil supply — driven in part by the expansion of U.S. shale production — caused a collapse to below \$30 in 2016. Although a partial recovery lifted prices into the \$50–70 range through 2019, the COVID-19 pandemic triggered a sharp demand shock, briefly reducing Brent crude oil prices to around \$20. A swift rebound followed. By 2021, prices had exceeded \$80, and Russia's invasion of Ukraine in 2022 drove them above \$120. Since then, oil prices have fluctuated mainly between \$70 and \$90 per barrel, a range shaped by ongoing geopolitical tensions and intensified speculative activity. Notably, extreme price changes frequently exceed 10% or even 20%. Overall, returns appear excessively large, and volatility tends to cluster.

4.2. Stochastic model dynamics

We now consider that oil demand is subject to shocks arising from business cycle fluctuations, whereas oil supply is affected by disruptions linked to production-related factors. See Kilian (2009), Gong et al. (2020), and Harrison et al. (2023) for evidence. Both demand and supply shocks are modeled as fundamental shocks and are specified as first-order autoregressive processes to capture their temporal persistence. Specifically, we enrich the demand for oil in (2) as

$$D_{t+1}:=a_{t+1}-bP_{t+1}, \tag{41}$$

where

$$a_{t+1}:=\bar{a}+\epsilon^{D}_{t+1}, \tag{42}$$

[9] See https://fred.stlouisfed.org/series/DCOILBRENTEU.

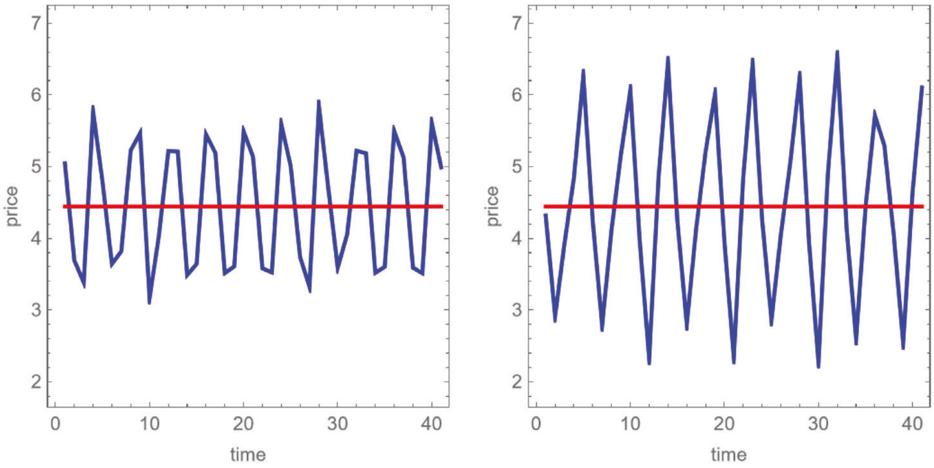

Fig. 15. Behavioral model extensions. Left panel: Switching between an extrapolative and a regressive expectation rule, based on $\beta = 1.85$, $e = 0.25$, and $f = 0.1$. Right panel: Switching between a trend-extrapolative and a regressive expectation rule, based on $\beta = 1.05$, $e = 0.25$, and $f = 0.1$. Remaining parameters: $a = 10$, $b = 1$, $c = 1.25$, $h = 1$, and $\alpha = 1$.

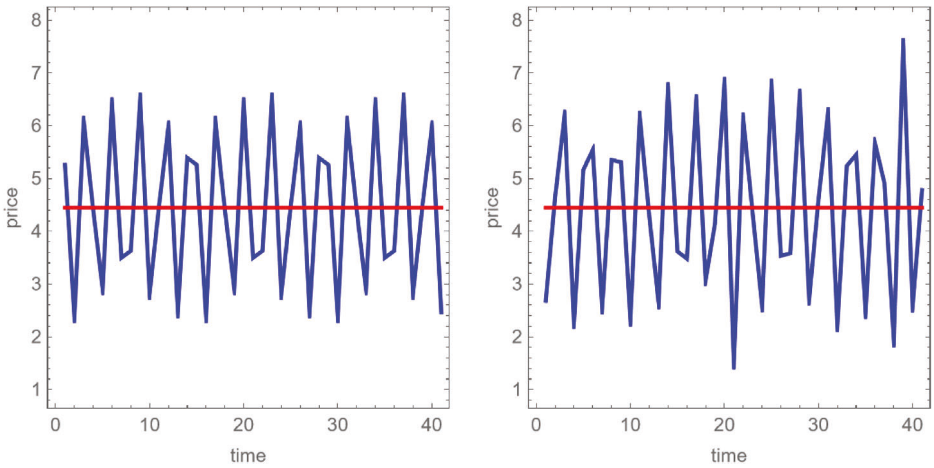

Fig. 16. Extrapolative expectations. Left panel: Periodic dynamics, obtained for $\beta = 0.35$. Right panel: Chaotic dynamics, obtained for $\beta = 1.05$. Remaining parameters: $a = 10$, $b = 1$, $c = 1.25$, $h = 1$, and $\alpha = 1$.

with

$$\epsilon^D_{t+1} := \rho^D \epsilon^D_t + \eta^D_{t+1}, \tag{43}$$

and the supply of oil in (6) as

$$S_{t+1} := c_t P_t, \tag{44}$$

where

$$c_t := \bar{c} + \epsilon^S_t, \tag{45}$$

with

$$\epsilon^S_t := \rho^S \epsilon^S_{t-1} + \eta^S_t. \tag{46}$$

The shocks η^D_t and η^S_t are independent and identically distributed normal random variables with mean zero and standard deviations σ^D and σ^S. The autocorrelation parameters satisfy $0 < \rho^D < 1$ and $0 < \rho^S < 1$. Needless to say, a_{t+1} and c_t have to remain positive during simulations.

In the absence of speculators, the oil price evolves as

$$P_{t+1} = \frac{a_{t+1}}{b} - \frac{c_t}{b} P_t \tag{47}$$

and its fundamental value follows

$$F_{t+1} = \frac{a_{t+1}}{b + c_t}, \tag{48}$$

while the asymptotic (long-run) mean of the fundamental value results as $\bar{F} = \frac{\bar{a}}{b+\bar{c}}$.

Then, the oil market model with speculators can be expressed as the random dynamical system (see the Eq. (49) in Box V) where a_{t+1}, c_t and F_t evolve as described above.

We now consider two illustrative examples. The simulation depicted in Fig. 18 highlights the effects of demand shocks in the presence of coexisting attractors. It is based on the parameter setting $\bar{a} = 23.5$, $b = 1$, $\bar{c} = 1.35$, $d = 0.99$, $h = 1$, $\rho^D = 0.9999$, $\rho^S = 0$, $\sigma^D = 0.1$, and $\sigma^S = 0$. Demand shocks do not alter the stability properties of the underlying steady state of the model's deterministic skeleton, as discussed in Section 2. Moreover, this parameter setting corresponds to the simulation shown in Fig. 4, where an attracting period-three cycle coexists with a locally stable fixed point.

The blue line in the top panel of Fig. 18 depicts the evolution of 10,000 (daily) oil prices, while the red line shows their time-varying fundamental value. In the long run, the oil price fluctuates around $\bar{F} = 10$, though lasting deviations occur. The bottom panel reveals significant volatility outbursts triggered by switching between the two coexisting attractors. As is evident, the volatility of the oil price is substantially higher than justified by its fundamental value.

The simulation depicted in Fig. 19 examines the effects of supply shocks and is based on the parameter setting $\bar{a} = 1404$, $b = 1$, $\bar{c} = 1.7$,

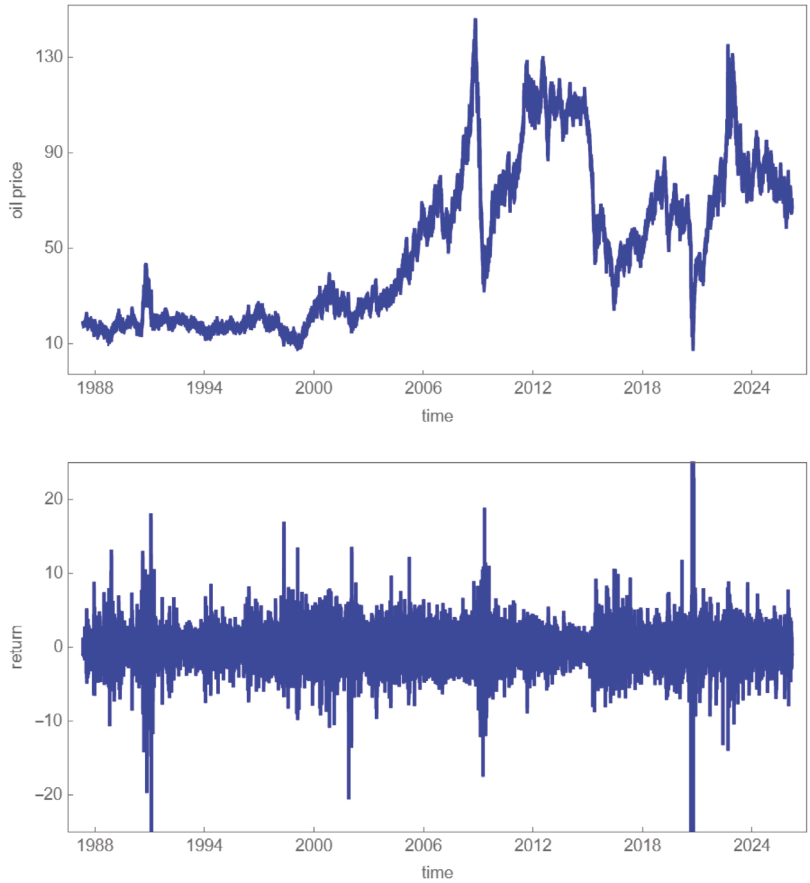

Fig. 17. Behavior of Brent crude oil prices. The top panel shows the evolution of daily oil prices from May 20, 1987, to August 31, 2025. The bottom panel displays the corresponding return dynamics. The time series, retrieved from the FRED database of the Federal Reserve Bank of St. Louis, comprises 9714 daily observations.

$$A' := \begin{cases} P_{t+1} = \begin{cases} -\frac{c_t}{b}P_t + \frac{a_{t+1}}{b} & \text{if} \quad h + d\left(P_t - F_t\right) \le 0 \wedge h + d\left(Y_t - F_{t-1}\right) \le 0 \\ -\frac{c_t}{b}P_t + \frac{a_{t+1}}{b} - \frac{d}{b}\left(Y_t - F_{t-1}\right) - \frac{h}{b} & \text{if} \quad h + d\left(P_t - F_t\right) \le 0 \wedge h + d\left(Y_t - F_{t-1}\right) > 0 \\ -\frac{c_t}{b}P_t + \frac{a_{t+1}}{b} + \frac{d}{b}\left(P_t - F_t\right) + \frac{h}{b} & \text{if} \quad h + d\left(P_t - F_t\right) > 0 \wedge h + d\left(Y_t - F_{t-1}\right) \le 0 \\ -\frac{c_t}{b}P_t + \frac{a_{t+1}}{b} + \frac{d}{b}\left(P_t - Y_t\right) & \text{if} \quad h + d\left(P_t - F_t\right) > 0 \wedge h + d\left(Y_t - F_{t-1}\right) > 0 \end{cases}, \\ \\ Y_{t+1} = P_t \end{cases} \tag{49}$$

Box V.

$d = 1.1$, $h = 1$, $\rho^D = 0$, $\rho^S = 0.999$, $\sigma^D = 0$, and $\sigma^S = 0.01$. For this set of parameter values, the deterministic skeleton ($\sigma^D = \sigma^S = 0.00$) of the model exhibits chaotic-type transient dynamics and cyclical long-run dynamics. In this case, supply shocks do affect the stability properties of the underlying steady state of the model's deterministic skeleton, as discussed in Section 2. In particular, the model's bifurcation structure as well as the amplitude of the attractors' oil price fluctuations depends on the parameter $\bar{c}$. As before, the blue line in the top panel of Fig. 19 depicts the path of 10,000 (daily) oil prices, while the red line shows their time-varying fundamental values. The asymptotic (long-run) mean of the fundamental value is now $\bar{F} = 520$. Once again, lasting fluctuations occur around this value, associated with significant volatility outbursts. As in the case of demand shocks, the volatility of the oil price is considerably higher than that of its fundamental value.

4.3. A statistical comparison of actual and simulated oil prices

We conclude this section by comparing key summary statistics of actual and simulated oil prices. Table 1 reports the minimum return, the maximum return, the mean absolute return, the kurtosis, and the autocorrelation coefficients of absolute returns at lags 5, 25, 50, and 100. The first row refers to Brent crude oil prices, the second row to WTI crude oil prices, and the third row to the simulated data depicted in Fig. 19.[10]

Overall, Table 1 suggests that the model is able to reproduce several key stylized facts of oil price dynamics. While the simulated return

[10] The WTI time series is also taken from FRED (series DCOILWTICO). We exclude the observation for April 20, 2020, when the WTI crude oil price turned negative.

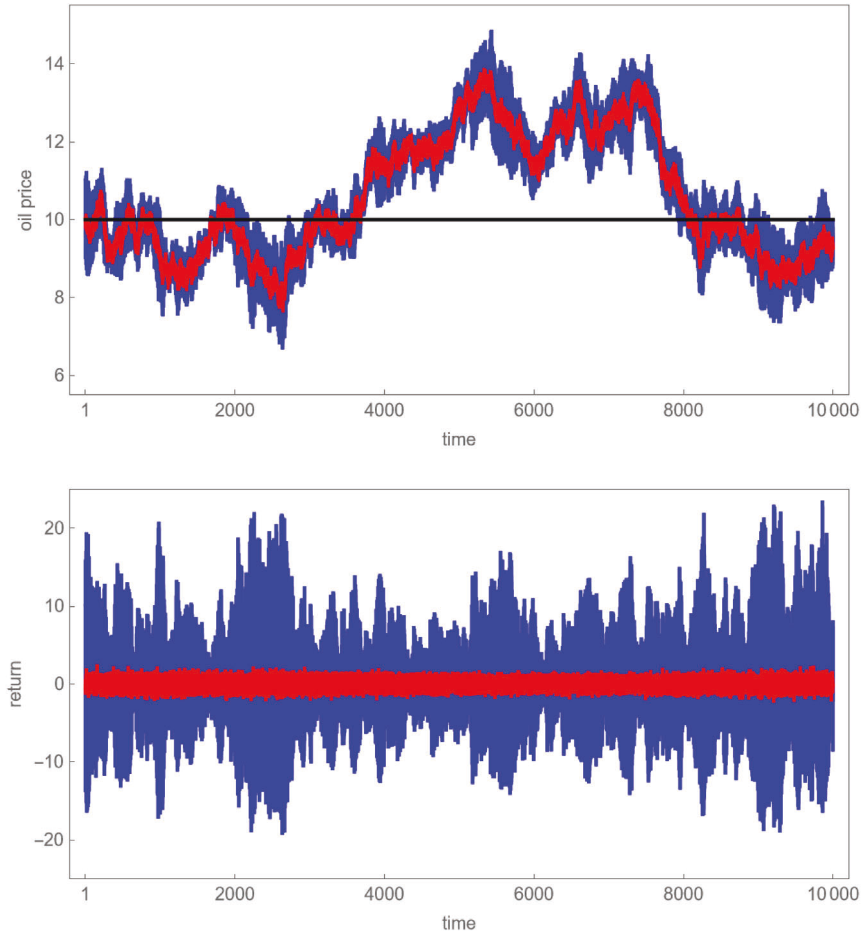

Fig. 18. Effects of demand shocks. The blue and red lines in the top panel depict the evolution of 10,000 (daily) oil prices and their fundamental values. The bottom panel shows the corresponding return dynamics. Parameter setting: $\bar{a} = 23.5$, $b = 1$, $\bar{c} = 1.35$, $d = 0.99$, $h = 1$, $\rho^D = 0.9999$, $\rho^S = 0$, $\sigma^D = 0.1$, and $\sigma^S = 0$. (For interpretation of the references to color in this figure legend, the reader is referred to the web version of this article.)

series generates substantial positive and negative returns, the magnitude of extreme movements remains somewhat below that observed for Brent and WTI. At the same time, the simulated returns exhibit excess kurtosis that is well above the Gaussian benchmark of 3 and thus consistent with fat-tailed behavior. Hence, both the empirical and simulated return series depart from normality, although the model produces less pronounced tail behavior. Importantly, the autocorrelation coefficients of absolute returns are broadly in line with their empirical counterparts. The model reproduces the slow decay pattern across lags 5, 25, 50, and 100, indicating that it captures volatility clustering in qualitative terms. Future work may seek to bring the model even closer to the empirical distributional properties of oil price returns. As a final takeaway, the calibration exercise highlights the need to combine shocks with nonlinear (cyclical or chaotic) dynamics in order to generate empirically consistent statistics for simulated oil price dynamics.

Table 1
Summary statistics of actual and simulated oil price returns. The table reports the minimum return $r_{\min}$, maximum return $r_{\max}$, mean absolute return $|r|$, kurtosis k, and autocorrelation coefficients of absolute returns at lags 5, 25, 50, and 100 (AC5–AC100). The first row refers to Brent crude oil prices, the second row to WTI crude oil prices, and the third row to the simulated data (using the same parameter values as in Fig. 19).

	$r_{\min}$	$r_{\max}$	$\|r\|$	k	AC5	AC25	AC50	AC100
Brent	−64.4	41.2	1.64	68.2	0.21	0.13	0.07	0.03
WTI	−72.0	42.6	1.75	76.1	0.22	0.14	0.05	0.04
Model	−19.2	25.1	2.51	8.35	0.25	0.17	0.07	0.04

5. Conclusions

Oil plays a central role in the global economy as a key input in production, heating, and transportation, while at the same time being a major driver of greenhouse gas emissions and climate change. Despite its importance, the speculative dynamics of oil prices, which in turn affect oil consumption and production, remain poorly understood, and market fluctuations are often difficult to explain within standard frameworks (see, for instance, Kilian (2008) and Zeppini and van den Bergh (2020)). To shed light on these dynamics, we develop a novel stock-flow consistent model of the oil market populated by four types of agents: producers, consumers, speculators, and policymakers. Since oil is both produced and consumed in every period, we adopt a cobweb-type framework.

As is common in this line of research, producers' supply increases linearly with past oil prices, while consumers' demand decreases linearly with the current oil price. To capture the speculative component of oil price formation, we assume that speculators buy or sell oil in order to maintain a desired market position and to engage in cash-and-carry and reverse cash-and-carry arbitrage, which requires the ability to store oil. Stock-flow consistency implies that speculative positions cannot be negative. Policymakers may impose a tax on producers' oil revenues with the aim of reducing oil consumption by increasing its price. In each period, the oil price adjusts to clear the market. In the

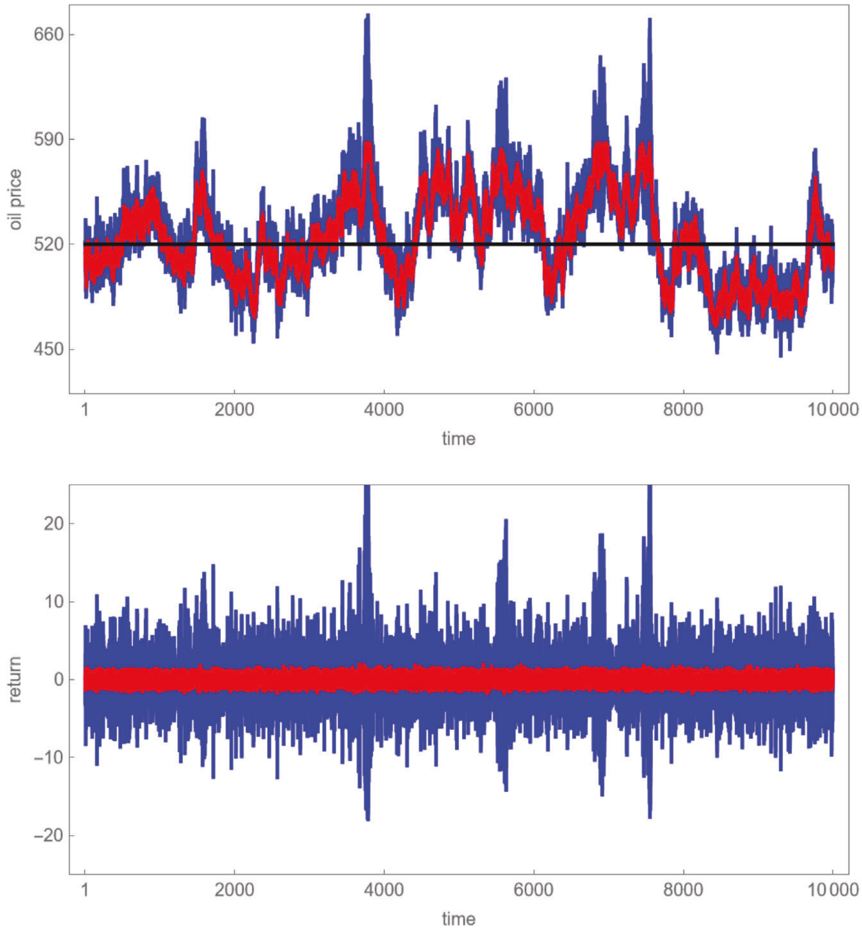

Fig. 19. Effects of supply shocks. The blue and red lines in the top panel depict the evolution of 10,000 (daily) oil prices and their fundamental values. The bottom panel shows the corresponding return dynamics. Parameter setting: $\bar{a} = 1404$, $b = 1$, $\bar{c} = 1.7$, $d = 1.1$, $h = 1$, $\rho^D = 0$, $\rho^S = 0.999$, $\sigma^D = 0$, and $\sigma^S = 0.01$. (For interpretation of the references to color in this figure legend, the reader is referred to the web version of this article.)

absence of speculators, the oil price follows a one-dimensional linear map. Since the steady-state price depends only on structural demand and supply parameters, we interpret it as the fundamental value of the oil market. Consistent with Ezekiel's (1938) Cobweb Theorem, the oil price converges to its fundamental value when the slope of the consumers' demand schedule exceeds that of the producers' supply schedule; otherwise, prices diverge. Our results further show that policymakers can raise the steady-state oil price, lower steady-state oil consumption, and enhance market stability by imposing higher tax rates on producers' oil revenues.

With speculators, however, the oil price in our baseline model is governed by a two-dimensional discontinuous piecewise-linear map. In this setting, oil prices may exhibit both regular and irregular fluctuations, regardless of the relative slopes of the demand and supply schedules. In other words, Ezekiel's (1938) Cobweb Theorem may no longer apply once speculation is introduced. In economic terms, the endogenous oil price dynamics generated by our model arise from the interaction of delayed production adjustments and speculative trend amplification. In the standard cobweb framework, producers react to past oil prices because production decisions are subject to time lags. High oil prices induce producers to expand future supply, while low prices discourage production. If these delayed supply responses are sufficiently strong relative to the price-dependent demand reactions of consumers, divergent zigzag price movements may emerge.

Importantly, our model reveals that the presence of speculators may fundamentally alter this mechanism. When oil prices rise above their fundamental level, speculators expect further price increases and expand their oil positions by purchasing and storing additional oil. This additional demand keeps prices relatively high, thereby preventing the sharper price declines that would occur in a standard cobweb model. Conversely, when oil prices fall, speculators reduce their positions or liquidate inventories. The resulting additional supply compensates for the low oil supply provided by producers and prevents the sharper price increases that would otherwise emerge in a standard cobweb model. By behaving procyclically, speculators absorb excess supply during downturns and excess demand during upswings, thereby preventing explosive price divergence and stabilizing an otherwise unstable market environment.

The interaction between delayed production responses and speculative inventory adjustments creates a mixture of negative and positive feedback loops that may generate persistent endogenous fluctuations. From this perspective, oil market turbulence is not necessarily driven solely by exogenous shocks, but may also emerge endogenously from the nonlinear interaction of heterogeneous market participants and delayed adjustment processes, as demonstrated in our paper.

Our analysis further indicates that taxing producers' oil revenues provides policymakers with only limited control over oil market dynamics. While higher tax rates create a tendency — though not a guarantee — for the oil price to converge toward its fundamental value, or at least to display bounded dynamics, they cannot fully prevent divergence. Robustness checks confirm these findings. Even when an upper bound on speculative storage is introduced, both regular and irregular dynamics persist. The inclusion of demand and supply shocks reveals additional mechanisms capable of generating bubbles, crashes, and volatility outbursts. Fundamental shocks may induce persistent oil price swings accompanied by heightened volatility. Moreover, volatility outbursts may emerge from attractor-switching dynamics, local and global bifurcations, and changes in the amplitude of oil price attractors.

Our theoretical assessment of the limited stabilizing potential of oil taxation is broadly consistent with empirical findings from the energy policy literature. Cross-country evidence suggests that carbon pricing and fuel taxation reduce fossil fuel consumption and emissions, yet their effects on price dynamics are typically moderate. For example, Andersson (2019) shows that the Swedish carbon tax significantly reduced transport emissions without generating major distortions in fuel markets. Metcalf and Stock (2023) find that carbon pricing schemes in Europe achieved measurable environmental effects with limited macroeconomic side effects. More generally, studies of fuel taxation across OECD countries (Bento et al., 2009) document that higher fuel taxes dampen consumption responses but do not eliminate exposure to global oil price fluctuations. At the same time, research on oil price volatility emphasizes the dominant role of global demand conditions and financial market forces (e.g., Kilian (2008) and Aastveit et al. (2015)), suggesting that national-level tax instruments can influence but not fully stabilize oil market dynamics. Taken together, this empirical evidence supports the view that taxation may contribute to greater stability through demand-side channels, while its quantitative impact remains inherently limited — an assessment that aligns with the mechanisms identified in our model.

Of course, our model rests on a number of simplifying assumptions. We briefly explored several extensions, including longer production lags, more sophisticated expectation-formation schemes, and a framework with heterogeneous, interacting speculators, providing illustrative examples for each case. These extensions suggest that the qualitative mechanisms identified in our baseline model remain relevant in richer environments. Future research may therefore study the dynamical systems associated with such model extensions in greater detail and systematically analyze their stability properties, bifurcation structures, and potential routes to complex dynamics. We deliberately opted for a parsimonious baseline setup in order to derive clear-cut insights into the functioning of the oil market. The stability and bifurcation analysis presented in this paper, together with the proof that the irregular behavior of simulated oil price fluctuations is indeed chaotic, illustrate the analytical advantages of such an approach. Further work is needed to deepen our understanding of oil price dynamics and to identify policy tools capable of stabilizing oil market fluctuations while simultaneously controlling oil consumption.

CRediT authorship contribution statement

Laura Gardini: Writing – review & editing, Writing – original draft, Visualization, Validation, Supervision, Software, Resources, Project administration, Methodology, Investigation, Formal analysis, Data curation, Conceptualization. **Davide Radi:** Writing – review & editing, Writing – original draft, Visualization, Validation, Supervision, Software, Resources, Project administration, Methodology, Investigation, Formal analysis, Data curation, Conceptualization. **Iryna Sushko:** Writing – review & editing, Writing – original draft, Visualization, Validation, Supervision, Software, Resources, Project administration, Methodology, Investigation, Formal analysis, Data curation, Conceptualization. **Frank Westerhoff:** Writing – review & editing, Writing – original draft, Visualization, Validation, Supervision, Software, Resources, Project administration, Methodology, Investigation, Formal analysis, Data curation, Conceptualization.

Acknowledgments

The work of Davide Radi and Iryna Sushko has been funded by the European Unione - Next Generation EU, Missione 4: "Education and Research" - Componente 2: "From research to business", through PRIN 2022 under the Italian Ministry of University and Research (MUR). Project: 2022JRY7EF - Qnt4Green - Quantitative Approaches for Green Bond Market: Risk Assessment, Agency Problems and Policy Incentives - CUP: J53D23004700008. Moreover, support from the VŠB-Technical University of Ostrava (SGS Research Project SP2026/003), and the European Union (REFRESH Project – Research Excellence for Region Sustainability and High-Tech Industries of the European Just Transition Fund, Grant CZ.10.03.01/00/22 003/0000048 via the Operational Programme Just Transition) is acknowledged. Finally, we thank the Gruppo Nazionale di Fisica Matematica GNFM-INdAM for financial support.

Appendix A. Technical proofs

Proof of Proposition 1. Property (1) follows by the definition of the map which requires $y_{t+1} = x_t$. Hence, equilibrium conditions $x_{t+1} = x_t = x$ and $y_{t+1} = y_t = y$ imply $x = y$. In regions $\mathcal{B}_1$, resp. $\mathcal{B}_3$, we have that x_{t+1} and y_{t+1} are functions of x_t only with $y_{t+1} = x_t$ and $x_{t+1} = -\frac{c}{b}x_t$, resp. $x_{t+1} = -\frac{c-d}{b}x_t + \frac{h}{b}$. Hence, $x_{t+1} = -\frac{c}{b}y_{t+1}$, resp. $x_{t+1} = -\frac{c-d}{b}y_{t+1} + \frac{h}{b}$, for all t, and properties (2) and (3) follow. Regarding properties (4)–(7), note that inside each one of the regions in which the state space is partitioned, say $\mathcal{B}_1$, $\mathcal{B}_2$, $\mathcal{B}_3$ and $\mathcal{B}_4$, map B is linear; hence, at most an (isolated) equilibrium can exist. The equilibria follows by imposing $x_{t+1} = x_t = \bar{x}$ and noting that $y_{t+1} = x_t = \bar{x}$. Regarding the local stability of the equilibria, we proceed by means of a standard eigenvalue analysis. In $\mathcal{B}_1$, the Jacobian is

$$J_1 = \begin{bmatrix} -\frac{c}{b} & 0 \\ 1 & 0 \end{bmatrix} \tag{A.1}$$

Hence, the eigenvalues are $\lambda_1^{\mathcal{B}_1} = -\frac{c}{b}$ and $\lambda_2^{\mathcal{B}_1} = 0$. Note that c and b are non-negative by assumption. Thus, imposing the sufficient conditions for local stability, that is, $-1 < \lambda_1^{\mathcal{B}_1}, \lambda_2^{\mathcal{B}_1} < +1$, we have that the fixed point of the map that applies in $\mathcal{B}_1$, that is, $(0,0)$, is locally asymptotically stable when $(0 \leq) c < b$. In $\mathcal{B}_2$, the Jacobian is

$$J_2 = \begin{bmatrix} -\frac{c}{b} & -\frac{d}{b} \\ 1 & 0 \end{bmatrix} \tag{A.2}$$

The associated characteristic equation is

$$b\left(\lambda^{\mathcal{B}_2}\right)^2 + c\lambda^{\mathcal{B}_2} + d = 0 \tag{A.3}$$

that is, the eigenvalues are

$$\lambda_{1,2}^{\mathcal{B}_2} = \frac{-c \pm \sqrt{c^2 - 4bd}}{2b} \tag{A.4}$$

It follows that the eigenvalues are a pair of complex conjugate numbers for $d > \frac{c^2}{4b}$. Noting that $-\frac{c}{b}$ and $\frac{d}{b}$ are the trace and the determinant of the Jacobian J_2, respectively, by Schur stability conditions, see, e.g., Jury (1963), we have that the equilibrium is locally asymptotically stable if and only if

$$\begin{array}{rcl} 1 + \frac{c}{b} + \frac{d}{b} & > & 0 \\ 1 - \frac{c}{b} + \frac{d}{b} & > & 0 \\ \frac{d}{b} & < & 1 \end{array} \tag{A.5}$$

Noting that $c, b, d > 0$ by assumption, the first inequality in (A.5) is always satisfied, while the other two can be rewritten as

$$\begin{array}{rcl} c & < & b + d \\ d & < & b \end{array} \tag{A.6}$$

Hence, property (6) follows. In $\mathcal{B}_3$, the Jacobian is

$$J_3 = \begin{bmatrix} -\frac{c-d}{b} & 0 \\ 1 & 0 \end{bmatrix} \tag{A.7}$$

Hence, the eigenvalues are $\lambda_1^{\mathcal{B}_3} = -\frac{c-d}{b}$ and $\lambda_2^{\mathcal{B}_3} = 0$. Note that c, b and d are non-negative by assumption. Thus, imposing the sufficient conditions for local stability, that is, $-1 < \lambda_1^{\mathcal{B}_3}, \lambda_2^{\mathcal{B}_3} < +1$, we have that the fixed point of the map that applies in $\mathcal{B}_3$, that is, $(0,0)$, is locally asymptotically stable when $d-b < c < d+b$. Hence, property (7) follows. In $\mathcal{B}_4$, the Jacobian is

$$J_4 = \begin{bmatrix} -\frac{c-d}{b} & -\frac{d}{b} \\ 1 & 0 \end{bmatrix} \tag{A.8}$$

The associated characteristic equation is

$$b\left(\lambda^{\mathcal{B}_4}\right)^2 + (c-d)\,\lambda^{\mathcal{B}_4} + d = 0 \tag{A.9}$$

that is, the eigenvalues are

$$\lambda_{1,2}^{\mathcal{B}_4} = \frac{-(c-d) \pm \sqrt{(c-d)^2 - 4bd}}{2b} \tag{A.10}$$

It follows that the eigenvalues are a pair of complex conjugate numbers for $d > \frac{(c-d)^2}{4b}$. Noting that $-\frac{c-d}{b}$ and $\frac{d}{b}$ are the trace and the determinant of the Jacobian J_2, respectively, by Schur stability conditions, see again Jury (1963), we have that the equilibrium is locally asymptotically stable if and only if

$$\begin{aligned} 1 + \frac{(c-d)}{b} + \frac{d}{b} &> 0 \\ 1 - \frac{(c-d)}{b} + \frac{d}{b} &> 0 \\ \frac{d}{b} &< 1 \end{aligned} \tag{A.11}$$

Noting that $c, b, d > 0$ by assumptions, the first inequality in (A.11) is always satisfied, while the other two can be rewritten as $c < b+2d$ and $b > d$. Hence, property (7) follows. Property (8) follows from properties (1), (4) and (7). ■

Proof of Proposition 2. The map D in (24) requires $y_{t+1} = x_t$. Hence, an equilibrium is a point in the straight line $x = y$. It follows that if an equilibrium exists, it is in one of the following regions D_1, D_5 and D_9. Imposing the equilibrium condition, that is, $x_{t+1} = x_t = x$ and $y_{t+1} = y_t = y$, on the maps that apply in D_1, D_5 and D_9, we always obtain $(0,0)$. It is straightforward to verify that $(0,0) \in D_5$. Hence, $(0,0) \notin D_1, D_9$. Hence, the local stability of the unique equilibrium $(0,0)$ is given by the Jacobian matrix of the map that applies in D_5. This map is the same as the one that applies in the region B_4 of the state space of model (21). Moreover, the same parameters' values restrictions apply. Hence, the stability condition follows from Proposition 1-(7). ■

Appendix B. Chaotic oil market dynamics

This technical appendix demonstrates that the oil-market model is capable of generating chaotic dynamics. Consider, for instance, the numerical example shown in Fig. 3. Since every point in region $\mathcal{B}_1$ is mapped onto the line defined by the equation $y = -\frac{b}{c}x$, any attractor that has at least one point in region $\mathcal{B}_1$ must have a portion that lies along this invariant line (for region $\mathcal{B}_1$).

Fig. B.20 (left panel) displays the same attractor as in Fig. 3; however, the portion of the attractor that lies along the invariant line $y = -\frac{b}{c}x$ is highlighted in orange. Exploiting this structure, we construct the associated first return map, shown in the right panel of Fig. B.20.

As can be seen, the first return map — denoted by f — is a piecewise smooth, non-invertible map. This map features two expanding (unstable[11]) fixed points, which we denote by p and q. Inside the absorbing interval marked by two black dots in Fig. B.20 we can see that the map consists in two segments, both with slope in modulus larger than 1. Thus, the dynamics are bounded and no attracting cycle can exist. The existing fixed points are homoclinic. In fact, the staircase diagram reveals the existence of a non-critical homoclinic orbit to p, denoted by $\mathcal{O}(p)$; see Definition 4 in Gardini et al. (2011). According to Theorem 2 in the same reference, in any neighborhood of $\mathcal{O}(p)$, there exists an invariant Cantor-like set Λ on which f exhibits chaotic dynamics. Also the fixed point q is expanding and it is easy to detect homoclinic orbits of q.

This confirms that the attractor shown in Fig. 3 is indeed chaotic, and thus, the oil-market model is capable of generating chaotic behavior.

Following a similar procedure and reasoning, it can be shown that the attractor in Fig. 5 is chaotic. Specifically, the left panel of Fig. B.21 highlights a portion of the attractor from Fig. 5 that lies along the invariant line of equation $y = \frac{bx-h}{d-c}$.[12] Using numerical techniques, it is possible to construct the first-return map on a segment of that critical line. This one-dimensional map is depicted in the right panel of Fig. B.21. A graphical inspection indicates that this map is also chaotic, although no visible homoclinic fixed points are present. In fact, all slopes of the 1D first return map within the absorbing interval have a modulus ≥ 1, so that the dynamics are bounded and the map cannot have any attracting cycle.

By applying similar methods, one can verify the presence of chaotic dynamics in any other numerical example reported in this paper where the existence of a chaotic attractor is specified.

Appendix C. An alternative mean–variance derivation of speculators' optimal short-term position in the oil market

Here, we provide an alternative derivation of the optimal short-term speculative position in the oil market given in (17). Consider traders who operate only in the spot oil market. Traders' profits from their short-term position depend on changes in the oil price: an increase (decrease) in the oil price raises (reduces) the value of their position. This can be formalized as follows:

$$\pi_{t+2} = \left(P_{t+2} - P_{t+1}\right) z_{t+1} - f, \tag{C.1}$$

where the parameter $f > 0$ denotes fixed costs associated with these operations, while z_{t+1} represents the speculative position on oil at time $t+1$. As in the asset-pricing model of Brock and Hommes (1998), speculators are assumed to be myopic mean–variance maximizers. Their optimal short-term speculative position is obtained from

$$\tilde{\delta}_{t+1} = \arg\max_{z_{t+1}} E_{s,t}\left[\pi_{t+2}\right] - \frac{\alpha}{2} V_{s,t}\left[\pi_{t+2}\right]. \tag{C.2}$$

Accordingly, speculators' optimal short-term position in the oil market is given by

$$\tilde{\delta}_{t+1} = \frac{E_{s,t}\left[P_{t+2} - P_{t+1}\right]}{\alpha V_{s,t}\left[P_{t+2} - P_{t+1}\right]}. \tag{C.3}$$

Speculators therefore take larger positions when they expect stronger oil price increases and smaller (or even negative) positions when perceived market risk is higher. Holding the price expectation rule $E_{s,t}\left[P_{t+2} - P_{t+1}\right]$ fixed, for instance as specified in (16), and assuming, as is standard in the heterogeneous-agent literature (see, e.g., Brock and Hommes (1998)), that speculators' variance beliefs are constant,

$$V_{s,t}\left[P_{t+2} - P_{t+1}\right] = \sigma^2. \tag{C.4}$$

the short-run speculative position in (17) is recovered by setting $d = \frac{\beta}{\alpha\sigma^2} > 0$.

[11] For a one-dimensional map, the notions of unstable and expanding fixed point coincide. Indeed, a fixed point is expanding if all eigenvalues of the derivative at that point have modulus greater than 1, see Gardini et al. (2011).

[12] This is the invariant line spanned by the eigenvector corresponding to an eigenvalue of the Jacobian of B in $\mathcal{B}_3$ and passing through its fixed point. It is invariant in $\mathcal{B}_3$; that is, every point of $\mathcal{B}_3$ is mapped onto this line in a single iteration. This line is also referred to as the critical line.

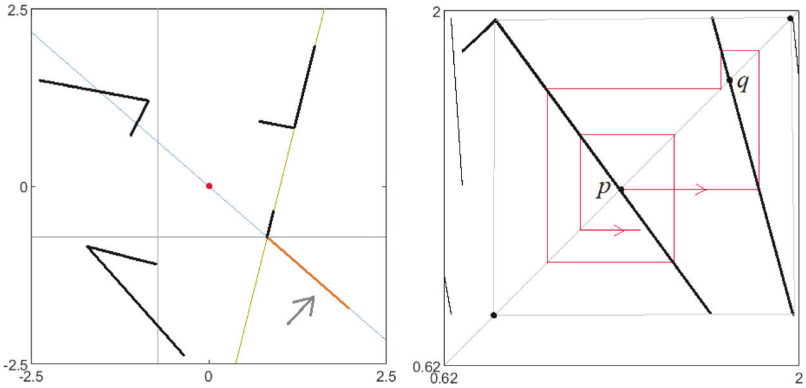

Fig. B.20. Left panel: state space with the chaotic attractor in black and the fundamental equilibrium in red. In blue the line of equation $y = -\frac{b}{c}x$, in yellow the line of equation $y = \frac{bx-h}{d-c}$. Right panel: first return map constructed on the red portion of the chaotic attractor depicted in the left panel. Parameters: $b = 1$, $c = 1.15$, $d = 1.4$, and $h = 1$. (For interpretation of the references to color in this figure legend, the reader is referred to the web version of this article.)

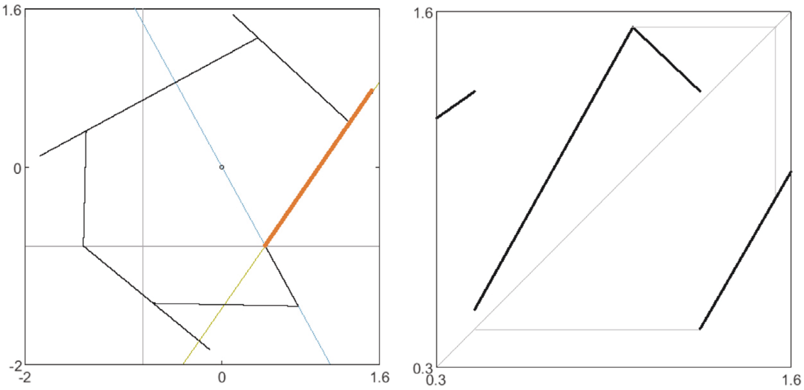

Fig. B.21. Left panel: state space with the chaotic attractor in black and the fundamental equilibrium in red. In blue the line of equation $y = -\frac{b}{c}x$, in yellow the line of equation $y = \frac{bx-h}{d-c}$. Right panel: first return map constructed on the red portion of the chaotic attractor depicted in the left panel. Parameters: $b = 1$, $c = 0.55$, $d = 1.25$, and $h = 1$. (For interpretation of the references to color in this figure legend, the reader is referred to the web version of this article.)

Appendix D. Learning-based foundation of the extrapolative expectations rule

Here, we show how to derive the extrapolative rule in (40) for speculators' oil price expectations within a heterogeneous expectations framework. We allow speculators to hold heterogeneous beliefs regarding future oil prices and, consequently, the shape of the forward curve. Although some speculators expect the forward curve to remain anchored to this fundamental benchmark, others anticipate temporary departures from it. These departures arise because market participants interpret deviations in the past spot oil price. Some speculators regard such deviations as transitory, whereas others view them as informative signals about future market conditions and extrapolate current price movements into the future. As a result, heterogeneous beliefs (forecasting rules) emerge regarding both future oil prices and the configuration of the forward curve.

We further assume an adaptive learning mechanism through which speculators continuously evaluate the performance of alternative forecasting rules. As forecast outcomes are realized, speculators revise their beliefs by assessing the historical accuracy of competing prediction strategies and gradually reallocate toward those that have performed relatively better. Consequently, the distribution of beliefs evolves endogenously over time in response to the relative success of alternative forecasting rules. To formalize this mechanism, we assume that speculators are grouped according to their forecasting rules, where type h is characterized by a belief about the oil price deviation, denoted by b_h, drawn from a general distribution of beliefs. The population share of each forecasting type evolves over time according to a discrete-choice framework with multinomial logit probabilities (Manski and McFadden, 1981). Accordingly, the fraction of speculators adopting forecasting rule h at time $t+1$ is given by

$$n_{t+1,h} = \frac{1}{Z_t} \exp[\gamma U_{t,h}], \tag{D.1}$$

where $Z_t = \sum_{h=1}^{H} \exp[\gamma U_{t,h}]$ is the normalization constant, H denotes the number of forecasting types, $U_{t,h}$ measures the past performance of forecasting rule h, defined as the negative squared forecast error, and $\gamma \geq 0$ is the intensity-of-choice parameter. Higher values of γ imply that speculators respond more strongly to differences in forecasting performance. Aggregate expectations of future oil-price changes are obtained as the weighted average of individual forecasts,

$$\bar{E}_{s,t+1}\left[P_{t+2} - P_{t+1}\right] = \sum_{h=1}^{H} b_h n_{t+1,h} = \frac{1}{Z_t} \sum_{h=1}^{H} b_h \exp\left[-\gamma\left(P_t - P_{t-1} - b_h\right)^2\right]. \tag{D.2}$$

For any finite H, this equation can be written as

$$\bar{E}_{s,t+1}\left[P_{t+2} - P_{t+1}\right] = \frac{\frac{1}{H}\sum_{h=1}^{H} b_h \exp\left[-\gamma\left(P_t - P_{t-1} - b_h\right)^2\right]}{\frac{1}{H}\sum_{h=1}^{H} \exp\left[-\gamma\left(P_t - P_{t-1} - b_h\right)^2\right]}. \tag{D.3}$$

Let us adopt the large-type limit (LTL) framework of Brock et al. (2005), where $H \to \infty$ and sample means are replaced by population means. Moreover, let b_h be normally distributed with mean zero and variance

s^2. Within this LTL framework, the dynamics for (D.3) are then given by[13]:

$$\bar{E}_{s,t+1}\left[P_{t+2}-P_{t+1}\right]=\frac{\int_{-\infty}^{+\infty} b\exp\left[-\gamma\left(P_t-P_{t-1}-b\right)^2\right]\exp\left[-b^2/(2s^2)\right]\mathrm{d}b}{\int_{-\infty}^{+\infty} \exp\left[-\gamma\left(P_t-P_{t-1}-b\right)^2\right]\exp\left[-b^2/(2s^2)\right]\mathrm{d}b}. \tag{D.4}$$

Using standard calculations (see, e.g., Appendix C in Hommes and Lustenhouwer (2019)), aggregate oil-price expectations in (D.4) simplify to

$$\bar{E}_{s,t+1}\left[P_{t+2}-P_{t+1}\right]=\beta\left(P_t-P_{t-1}\right), \tag{D.5}$$

where the extrapolation rate $\beta\in(0,1]$ is defined as

$$\beta=\frac{2\gamma s^2}{1+2\gamma s^2}. \tag{D.6}$$

The extrapolation rate measures the sensitivity of the oil forward curve to past spot price deviations. For a given intensity of choice γ, lower dispersion of beliefs implies lower values of β. In the limiting case $s^2\to 0$, the extrapolation rate converges to zero. In contrast, as the dispersion of belief increases, expectations become progressively more responsive to past price movements and β approaches one.

[13] According to this expectation formation mechanism, the expected oil price may also become negative. This phenomenon has been observed in practice, for example during the 2020 pandemic crisis, due to storage costs and other market-specific frictions. Moreover, the same aggregate expectation scheme (D.4) can be derived by assuming a Bayesian updating belief mechanism, as shown in Hommes and Lustenhouwer (2019).

References

Aastveit, K., Bjørnland, H., Thorsrud, L., 2015. What drives oil prices? Emerging versus developed economies. J. Appl. Econometrics 30, 1013–1028.
Andersson, J., 2019. Carbon taxes and CO_2 emissions: Sweden as a case study. Am. Econ. J.: Econ. Policy 11, 1–30.
Anufriev, M., Tuinstra, J., 2013. The impact of short-selling constraints on financial market stability in a heterogeneous agents model. J. Econom. Dynam. Control 37, 1523–1543.
Artstein, Z., 1983. Irregular cobweb dynamics. Econom. Lett. 11, 15–17.
Avrutin, V., Gardini, L., Sushko, I., Tramontana, F., 2019. Continuous and Discontinuous Piecewise-Smooth One-Dimensional Maps. Vol. 95, World Scientific Series on Nonlinear Science Series A, Singapore.
Axtell, R., Farmer, D., 2025. Agent-based modeling in economics and finance: Past, present, and future. J. Econ. Lit. 63, 197–287.
Bento, A., Goulder, L., Jacobsen, M., von Haefen, R., 2009. Distributional and efficiency impacts of increased U.S. gasoline taxes. Am. Econ. Rev. 99, 667–699.
Brock, W., Hommes, C., 1998. Heterogeneous beliefs and routes to chaos in a simple asset pricing model. J. Econom. Dynam. Control 22, 1235–1274.
Brock, W., Hommes, C., Wagener, F., 2005. Evolutionary dynamics in markets with many trader types. J. Math. Econom. 41, 7–42.
Chiarella, C., 1988. The cobweb model: Its instability and the onset of chaos. Econ. Model. 5, 377–384.
Chiarella, C., 1992. The dynamics of speculative behavior. Ann. Oper. Res. 37, 101–123.
Cifarelli, G., Paladino, G., 2010. Oil price dynamics and speculation: A multivariate financial approach. Energy Econ. 32, 363–372.
Cutler, D., Poterba, J., Summers, L., 1990. Speculative dynamics and the role of feedback traders. Am. Econ. Rev. 80, 63–68.
Cutler, D., Poterba, J., Summers, L., 1991. Speculative dynamics. Rev. Econ. Stud. 58, 529–546.
Day, R., Huang, W., 1990. Bulls, bears and market sheep. J. Econ. Behav. Organ. 14, 299–329.
De Grauwe, P., Dewachter, H., Embrechts, M., 1993. Exchange Rate Theory: Chaotic Models of Foreign Exchange Markets. Blackwell Pub, Oxford.
di Bernardo, M., Budd, C., Champneys, A., Kowalczyk, P., 2008. Piecewise-smooth Dynamical Systems: Theory and Applications. Applied Matheamtical Sciences, vol. 163, Springer Verlag, London.
Dieci, R., Gardini, L., Westerhoff, F., 2022. On the destabilizing nature of capital gains taxes. Int. Rev. Financ. Anal. 83, 102258.
Dieci, R., He, X.-Z., 2018. Heterogeneous agent models in finance. In: Hommes, C., LeBaron, B. (Eds.), Handbook of Computational Economics. Vol. 4, North-Holland, Amsterdam, pp. 257–328, chapter 5.
Dieci, R., Westerhoff, F., 2010. Interacting cobweb markets. J. Econ. Behav. Organ. 75, 461–481.
Ederington, L., Fernando, C., Holl, K., Lee, T., Linn, S., 2021. Dynamics of arbitrage. J. Financ. Quant. Anal. 56, 1350–1380.
Ezekiel, M., 1938. The cobweb theorem. Q. J. Econ. 52, 255–280.
Froot, K., 1995. Hedging portfolios with real assets. J. Portf. Manag. 21, 60–77.
Gardini, L., Radi, D., Schmitt, N., Sushko, I., Westerhoff, F., 2025. On the limits of informationally efficient stock markets: New insights from a chartist-fundamentalist model. Int. Rev. Financ. Anal. 105, 104436.
Gardini, L., Schmitt, D., Sushko, I., Westerhoff, F., 2022. Currency manipulation and currency wars: Analyzing the dynamics of competitive central bank interventions. J. Econom. Dynam. Control 145, 104545.
Gardini, L., Sushko, I., Avrutin, V., Schanz, M., 2011. Critical homoclinic orbits lead to snap-back repellors. Chaos Solitons Fractals 44, 433–449.
Gong, X., Chen, L., Lin, B., 2020. Analyzing dynamic impacts of different oil shocks on oil price. Energy 198, 117306.
Harrison, A., Liu, X., Stewart, S., 2023. Structural sources of oil market volatility and correlation dynamics. Energy Econ. 121, 104589.
He, X.-Z., Westerhoff, F., 2005. Commodity markets, price limiters and speculative price dynamics. J. Econom. Dynam. Control 29, 1577–1596.
Hommes, C., 1991. Adaptive learning and roads to chaos: The case of the cobweb. Econom. Lett. 36, 127–132.
Hommes, C., 2013. Behavioral Rationality and Heterogeneous Expectations in Complex Economic Systems. Cambridge University Press, Cambridge.
Hommes, C., Lustenhouwer, J., 2019. Managing unanchored, heterogeneous expectations and liquidity traps. J. Econom. Dynam. Control 101, 1–16.
Jungeilges, J., Maklakova, E., Perevalova, T., 2021. Asset price dynamics in a "bull and bear market". Struct. Change Econ. Dyn. 56, 117–128.
Jungeilges, J., Maklakova, E., Perevalova, T., 2022. Stochastic sensitivity of bull and bear states. J. Econ. Interact. Coord. 17, 165–190.
Jury, E., 1963. On the roots of a real polynomial inside the unit circle and a stability criterion for linear discrete systems. In: IFAC Proceedings Volumes. Vol. 1, International Federation of Automatic Control (IFAC), pp. 142–153.
Kilian, L., 2008. The economic effects of energy price shocks. J. Econ. Lit. 46, 871–909.
Kilian, L., 2009. Not all oil price shocks are alike: Disentangling demand and supply shocks in the crude oil market. Am. Econ. Rev. 99, 1053–1069.
Leontief, W., 1934. Verzögerte angebotsanpassung und partielles gleichgewicht. Z. Für Nationalökonomie 5, 670–676.
Lin, B., Wesseh, Jr., P., Appiah, M., 2014. Oil price fluctuation, volatility spillover and the Ghanaian equity market: Implication for portfolio management and hedging effectiveness. Energy Econ. 42, 172–182.
Manski, C., McFadden, D., 1981. Structural Analysis of Discrete Data with Econometric Applications. The MIT Press, Cambridge.
Markowitz, H., 1952. Portfolio selection. J. Financ. 7, 77–91.
Metcalf, G., Stock, J., 2023. The macroeconomic impact of Europe's carbon taxes. Am. Econ. J.: Macroecon. 15, 265–286.
Neville, H., Draaisma, T., Funnell, B., Harvey, C., van Hemert, O., 2021. The best strategies for inflationary times. J. Portf. Manag. 47, 8–37.
Okorie, D., Lin, B., 2020. Crude oil price and cryptocurrencies: Evidence of volatility connectedness and hedging strategy. Energy Econ. 87, 104703.
Panchuk, A., Sushko, I., Westerhoff, F., 2018. A financial market model with two discontinuities: Bifurcation structures in the chaotic domain. Chaos: An Interdiscip. J. Nonlinear Sci. 28, 055908.
Reitz, S., Westerhoff, F., 2007. Commodity price cycles and heterogeneous speculators: A STAR–GARCH model. Empir. Econ. 33, 231–244.
Ricci, U., 1930. Die "synthetische Ökonomie" von henry ludwell moore. Z. Für Nationalökonomie 1, 649–668.
Schultz, H., 1930. Der Sinn der Statistischen Nachfragekurven. In: Veröffentlichungen der Frankfurter Gesellschaft für Konjunkturforschung, Vol. 10, Schroeder, Bonn.
Smales, L., 2021. Geopolitical risk and volatility spillovers in oil and stock markets. Q. Rev. Econ. Financ. 80, 358–366.
Sornette, D., Woodard, R., Zhou, W.-X., 2009. The 2006–2008 oil bubble: Evidence of speculation, and prediction. Phys. A 388, 1571–1576.
Sushko, I., Tramontana, F., 2025. Regular and chaotic dynamics in a 2D discontinuous financial market model with heterogeneous traders. Math. Comput. Simulation 230, 386–399.
ter Ellen, S., Hommes, C., Zwinkels, R., 2021. Comparing behavioural heterogeneity across asset classes. J. Econ. Behav. Organ. 185, 747–769.
ter Ellen, S., Zwinkels, R., 2010. Oil price dynamics: A behavioral finance approach with heterogeneous agents. Energy Econ. 32, 1427–1434.
Tinbergen, J., 1930. Bestimmung und deutung von angebotskurven: Ein beispiel. Z. Für Nationalökonomie 1, 669–679.
Tramontana, F., Westerhoff, F., Gardini, L., 2013. The bull and bear market model of Huang and Day: Some extensions and new results. J. Econom. Dynam. Control 37, 2351–2370.
Westerhoff, F., 2008. The use of agent-based financial market models to test the effectiveness of regulatory policies. Jahrbücher Für Nationalökonomie Und Stat. 228, 195–227.

Westerhoff, F., Franke, R., 2018. Agent-based models for economic policy design: Two illustrative examples. In: Chen, S.-H., Kaboudan, M., Du, Y.-R. (Eds.), The Oxford Handbook of Computational Economics and Finance. Oxford University Press, Oxford, pp. 520–558, chapter 18.
Zeppini, P., van den Bergh, J., 2020. Global competition dynamics of fossil fuels and renewable energy under climate policies and peak oil: A behavioural model. Energy Policy 136, 110907.
Zhang, Q., Hu, Y., Jiao, J., Wang, S., 2024. The impact of Russia-Ukraine war on crude oil prices: An EMC framework. Humanit. Soc. Sci. Commun. 11, 8.
Zhusubaliyev, Z., Mosekilde, E., 2003. Bifurcations and Chaos in Piecewise-Smooth Dynamical Systems. World Scientific, New Jersey.